1956-05

The determination of Longitudinal virtual mass and damping of a rotating propeller

Russell, Hubert Edward; Stancliff, Robert C.; White, Roderick MacLead

Massachusetts Institute of Technology

THE DETERMINATION OF LONGITUDINAL VIRTUAL MASS AND DAMPING OF A ROTATING PROPELLER

Hubert Edward Russell
Robert Claude Stancliff
and
Roderick Macleod White

THE DETERMINATION OF LONGITUDINAL VIRTUAL MASS AND DAMPING OF A ROTATING PROPELLER

by

HUBERT EDWARD RUSSELL, LIEUTENANT, U.S. COAST GUARD
B.S., U.S. Coast Guard Academy (1950)

and

ROBERT CLAUDE STANCLIFF, LIEUTENANT, U.S. COAST GUARD
B.S., U.S. Coast Guard Academy (1950)

and

RODERICK MACLEOD WHITE, LIEUTENANT, U.S. COAST GUARD
B.S., U.S. Coast Guard Academy (1950)

SUBMITTED IN PARTIAL FULFILLMENT
OF THE REQUIREMENTS FOR THE
DEGREE OF NAVAL ENGINEER

at the

MASSACHUSETTS INSTITUTE OF TECHNOLOGY

May 1956

Department of Naval Architecture and
Marine Engineering, May 21, 1956

Signature of Authors

Certified by:

Accepted by:

Chairman, Departmental Committee
on Graduate Students

Thesis

THE DETERMINATION OF LONGITUDINAL VIRTUAL MASS AND DAMPING OF A ROTATING PROPELLER

by

HUBERT EDWARD RUSSELL, LIEUTENANT, U.S. COAST GUARD

ROBERT CLAUDE STANCLIFF, LIEUTENANT, U.S. COAST GUARD

RODERICK MACLEOD WHITE, LIEUTENANT, U.S. COAST GUARD

Submitted to the Department of Naval Architecture and Marine Engineering on May 21, 1956 in partial fulfillment of the requirements for the degree of Naval Engineer.

ABSTRACT

The determination of the effective mass and the damping of marine propellers is essential to the analysis of the longitudinal vibrational characteristics of a ship's shafting system. Effective mass is the actual mass of the propeller plus a virtual mass due to entrained water vibrating with the propeller. Our object was to contribute to the solution of the general problem by making an experimental determination of the virtual mass under operating conditions. Damping was to be measured coincidently.

Propellers selected for testing included a set of merchant type propellers with P/D values ranging from 0.8 to 1.2 (4 bladed), a set of DD type propellers with a variation of P/D (4 bladed), and a set of DD type propellers with a variation of P/D (3 bladed). Operating conditions (in the MIT Propeller Tunnel) were attained by driving the propellers through a torque coupling having small longitudinal stiffness and maintaining appropriate water velocities. The propellers were supported by a shaft and housing which were principally supported by two sets of pairs of converging rods, so arranged as to allow longitudinal motion of the housing but constraint against any other movement. A step longitudinal displacement of the propeller and housing caused a transient vibration which was recorded using a strain-gage transducer and recorder. The primary longitudinal stiffness of the system was related to the stiffness of the rods in bending. A longitudinal stiffness constant was determined which related the mass of the whole system to the square of the natural period. Using this relationship the mass could be determined by observing the period of vibration. The original decay was measured from the tape record of the transient vibrations.

The virtual mass was determined for each propeller along with the damping. The data for virtual mass was corrected to account for the degree of torsional coupling. These data were correlated on the basis of four parameters, pitch ratio, diameter, mean width ratio, and number of blades.

The following conclusions were drawn:

1. $W'_{ersw} = 5.775 \left[(1.350-P/D)^2 + .228\right] \left(\frac{d}{10}\right)^3 N^{.8} \; MWR^{1.13}$ lbs. (1)

$0.75 \quad P/D \quad 1.25$

P/D = Pitch ratio
d = Propeller diameter (in.)
N = Number of blades
MWR = Mean width ratio

2. Virtual mass as a percentage of total weight of bronze propeller blades (blade thickness fraction = 0.05) is as follows:

P/D	4 Bladed Merchant	3 Bladed DD	4 Bladed DD
.9	71%	71%	72%
1.2	44%	41%	42%

3. Values of virtual weight under operating conditions were significantly less than static test values.

4. No consistent variation of virtual weight was apparent with a variation of J.

5. Damping factors were about 1/3 theoretical values.

The following recommendations were made:

1. Compare aluminum and bronze model propellers to investigate torsional coupling.

2. Run more propellers, including some of varying diameters.

3. Investigate damping more thoroughly.

4. Investigate variation of support longitudinal stiffness.

Thesis Supervisor: Frank M. Lewis

Title: Professor of Marine Engineering

ACKNOWLEDGEMENT

The authors wish to express their appreciation to the following:

Professor Frank M. Lewis, for intellectual guidance.

Raymond E. Johnson, for practical assistance.

Our Wives, for infinite patience.

Cambridge, Massachusetts
May 21, 1956

Secretary of the Faculty
Massachusetts Institute of Technology
Cambridge 39, Massachusetts

Dear Sir:

In accordance with the requirements of the degree of Naval Engineer, we herewith submit a thesis entitled "The Determination of Longitudinal Virtual Mass and Damping of a Rotating Propeller."

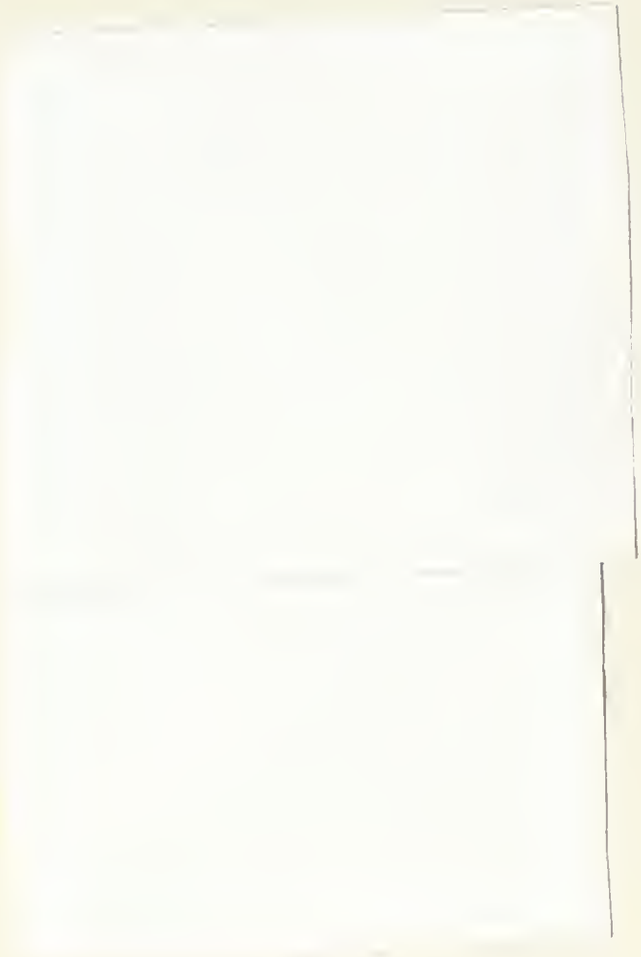

TABLE OF CONTENTS

TABLE OF FIGURES AND TABLES

TABLES

DEFINITIONS

B_a = Damping constant of propeller and support complete, $\frac{2\alpha W_a}{g}$ $\frac{(\text{lb sec})}{(\text{ft})}$

B_e = Damping constant of propeller, $B_a - B_s$ $\frac{(\text{lb sec})}{(\text{ft})}$

B_s = Damping constant of support $\frac{2\alpha(W_s + \text{wt of hub and entrained water})}{g}$ $\frac{(\text{lb sec})}{(\text{ft})}$

b = Simple theoretical damping constant, $\frac{\rho n D^3 dK_t}{dJ}$ $\frac{(\text{lb sec})}{(\text{ft})}$

C_I = Torsional coupling factor

D = Diameter of propeller, (ft)

d = Diameter of propeller, (in)

h = Height of bromo-benzene and water column (fine scale) for v_o computation, (mm)

h_{corr} = Corrected height of column due to temperature effect. (This is negligible in its application to the experiments but the correction is a characteristic of the MIT tunnel.) (mm)

I_p = Polar inertia, (lb sec^2 in)

J = Parameter of propeller operation, $\frac{v_o}{nD}$ (dimensionless)

K_t = Thrust coefficient, $\frac{(\text{thrust})}{\rho n^2 D^4}$. (dimensionless)

k_L = Longitudinal spring constant, $\frac{(\text{lb})}{(\text{in})}$

k_θ = Torsional spring constant, $\frac{(\text{in lb})}{(\text{rad})}$

N = Shaft revolutions per minute, (rpm)

n = Shaft revolutions per second, (rps)

P = Pitch of propeller, (ft)

p = Pitch of propeller, (in)

S = Slope of plot of W_a (or weight added) vs. T_n^2, $\frac{W_a}{T_n^2}$ $\frac{(lb)}{(sec^2)}$

T_o = Observed period of vibration, (sec)

T_n = Natural period of vibration. $T_n = \frac{T_o}{\sqrt{1 + \frac{a^2 T_o^2}{4\pi^2}}}$

t = Temperature of water in tunnel, (^oF)

v_o = Water velocity, propeller speed of advance. $0.41656\sqrt{h_{corr}}$ $\frac{(ft)}{(sec)}$

W_a = Apparent weight of propeller and support complete in water. (From period measurement), (lb)

$W_{a\,corr}$ = Apparent weight corrected to condition of infinite torsional stiffness of coupling C_I W_a (lb). (W_a as used in this equation was the W_a (average, operating) as tabulated in Tables III - XII)

W_e = Virtual weight of water entrained by blades, $W_e = W_a - W_l - W_s$ (lb)

W_e' = Virtual weight corrected to condition of infinite torsional stiffness of coupling, $W_e' = W_{a_{corrected}} - W_l - W_s$

W_h = Weight of water entrained within hub around shaft, (lb)

W_p = Weight of propeller, (lb)

W_s = Apparent weight of support in water including water entrained in housing, nose, and propeller drive collar. (From period measurement), (lb)

W_1 = Weight added to shaft in excess of nose and collar, $W_p + W_h$ (lb)

α = Reciprocal of time constant, exponential decay. $\frac{(1)}{(sec)}$

ρ = Density of medium. $\frac{(lb\ sec^2)}{(ft^4)}$

INTRODUCTION

The determination of the effective mass and the damping of marine propellers is essential to the analysis of the longitudinal vibrational characteristics of a ship's shafting system. By definition the effective mass consists of the actual mass of the propeller plus a virtual mass due to entrained water vibrating with the propeller. In the process of analyzing the shafting system it is necessary to make many engineering assumptions such as the degree of fixity at the thrust bearing, the amount of structure moving with the shaft at the forward end, the yielding of the ship's hull, the inertia of the water entrained by the hull, and the effective mass of the propeller. It was our object to contribute to the solution of the general problem by making a more accurate determination of this effective mass than has been made heretofore.

The only previous determination was with free-to-rotate non-driven propellers immersed in water and vibrated axially. (1)[1] Our apparatus was designed to determine the virtual mass of propellers under operating conditions, that is, rotating and delivering power. The method was such that it was also possible to measure propeller damping.

The basic instrumentation problem was to support the propeller so that it was free to vibrate longitudinally (along the propeller axis) and so that torque could be applied to drive the propeller. The support system as illustrated in Figures II-VI consists of a 12 inch section of 3/4 inch stainless steel shafting supported and longitudinally constrained by laminated bakelite bearings at each end of the bearing housing. This

[1] Numbers in parenthesis refer to references listed in the bibliography.

Figure I

Operating position adjacent to tunnel showing Sanborn Recorder, initial-displacement-wire, (arrow), and tunnel window for observation.

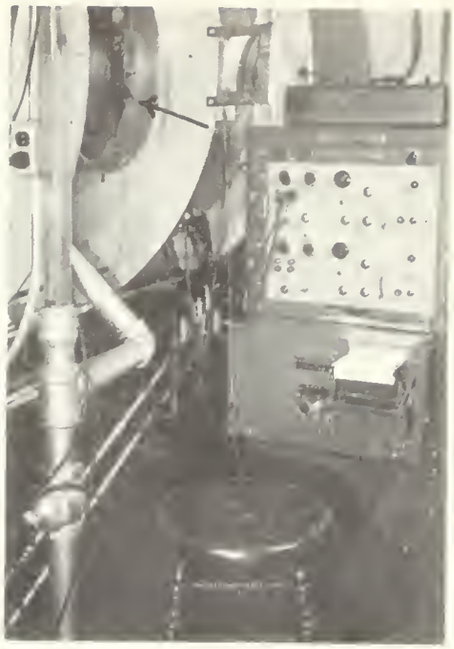

Figure II

Propeller (Merchant Type) in operating position. (Flow is left to right.) Note initial-displacement-wire and leads to strain gages on the nearest rod.

Figure III

Exploded view of apparatus showing three different propellers with associated collar (thrust) and nose assemblies.

Figure IV

Exploded view of apparatus showing collar and nose assemblies, thrust collar, torque coupling, shaft, support rods, and strain gages.

Figure V

Apparatus assembled except for propeller.

Figure VI

Apparatus assembled and installed in propeller tunnel (3 bladed DD409 Type Propeller) showing torque coupling and initial-displacement wire.

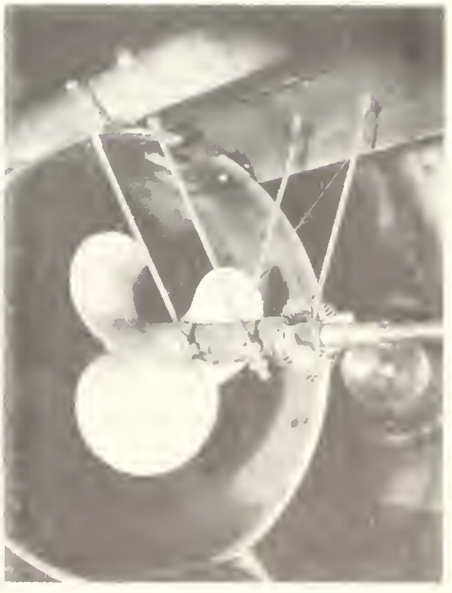

housing is a section of bronze pipe 5 inches long and 1.7 inch outside diameter which is itself supported by four 3/16 inch steel rods 12 inches long. The rods are bolted at their upper end to 6" x 2" channel beams rigidly secured in the propeller tunnel. A collar is keyed to the shaft and drives the propeller through dowels. A nose piece is screwed onto the shaft to seat against the propeller hub in order to hold the propeller securely against the collar and to fair the approaching water flow. To the driven end of this shaft a torque arm is keyed. This torque arm is driven by four springs connected to a similar torque arm on the driving shaft. The radius of the torque arm is 2 inches and the effective torque radius of the springs is 1.2 inches. Typical tested propellers are illustrated in Figure V.

Propellers having the greatest variation possible in pitch/diameter ratio and mean width ratio were selected for testing. One series consisted of five merchant type propellers, two bronze, three aluminum, having four blades, a MWR of .248, and having P/D ratios from .8 to 1.2. Five aluminum destroyer propellers of three and four blades with MWR of .458 and the same P/D range were selected for the second series. The propellers are further described in tables III to XIII in Appendix A.

To make observations the entire support system was excited by a step displacement from the steady state. The signal from an SR-4 strain gage transducer attached to one of the rods was the input to a Sanborn Recorder. The recorder produced a trace (see Figures VII and VIII) which is a measure of the instantaneous longitudinal position of the propeller. The time for each complete oscillation of the trace is the damped period of vibration of the system. This period may be simply

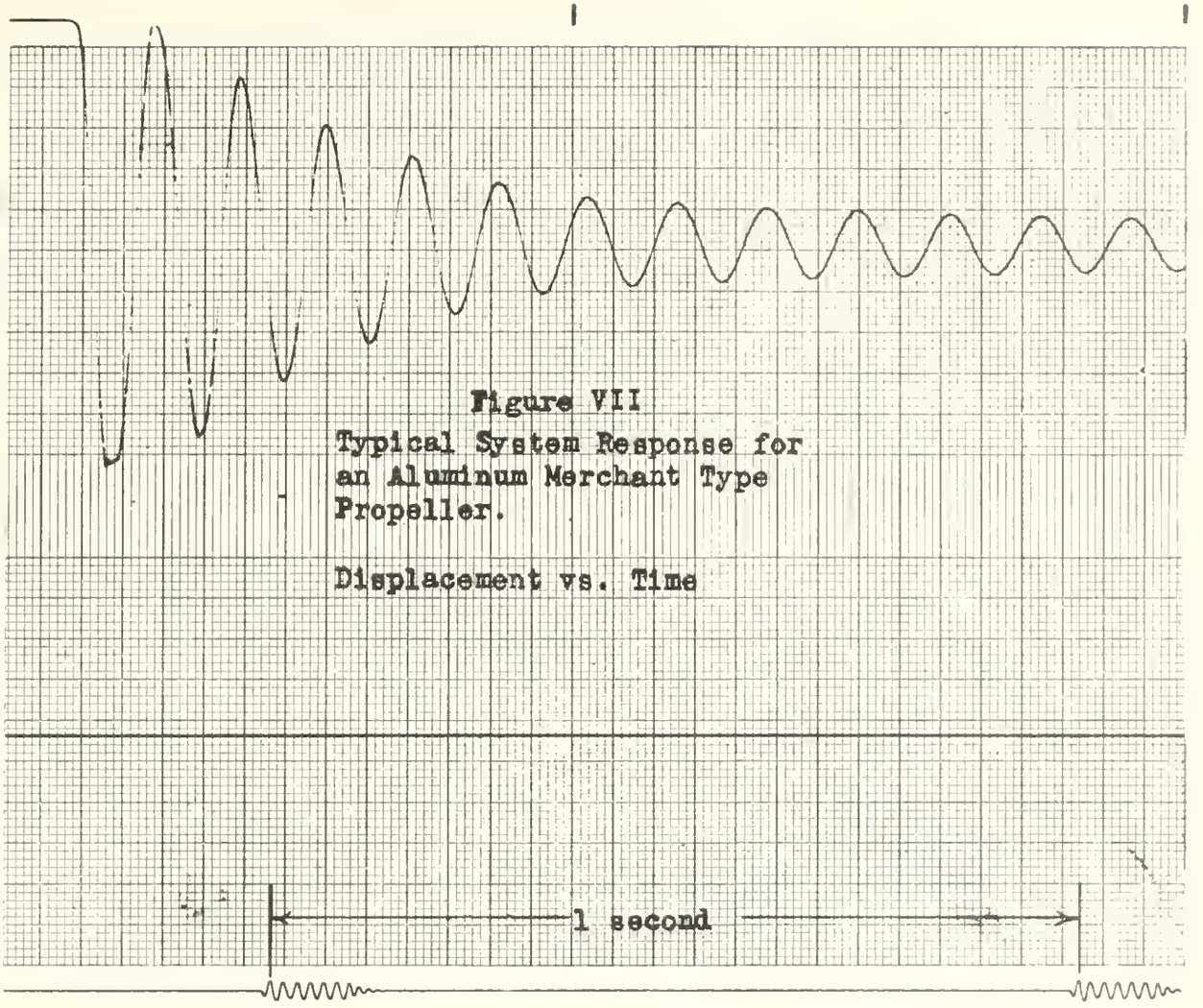

Figure VII

Typical System Response for an Aluminum Merchant Type Propeller.

Displacement vs. Time

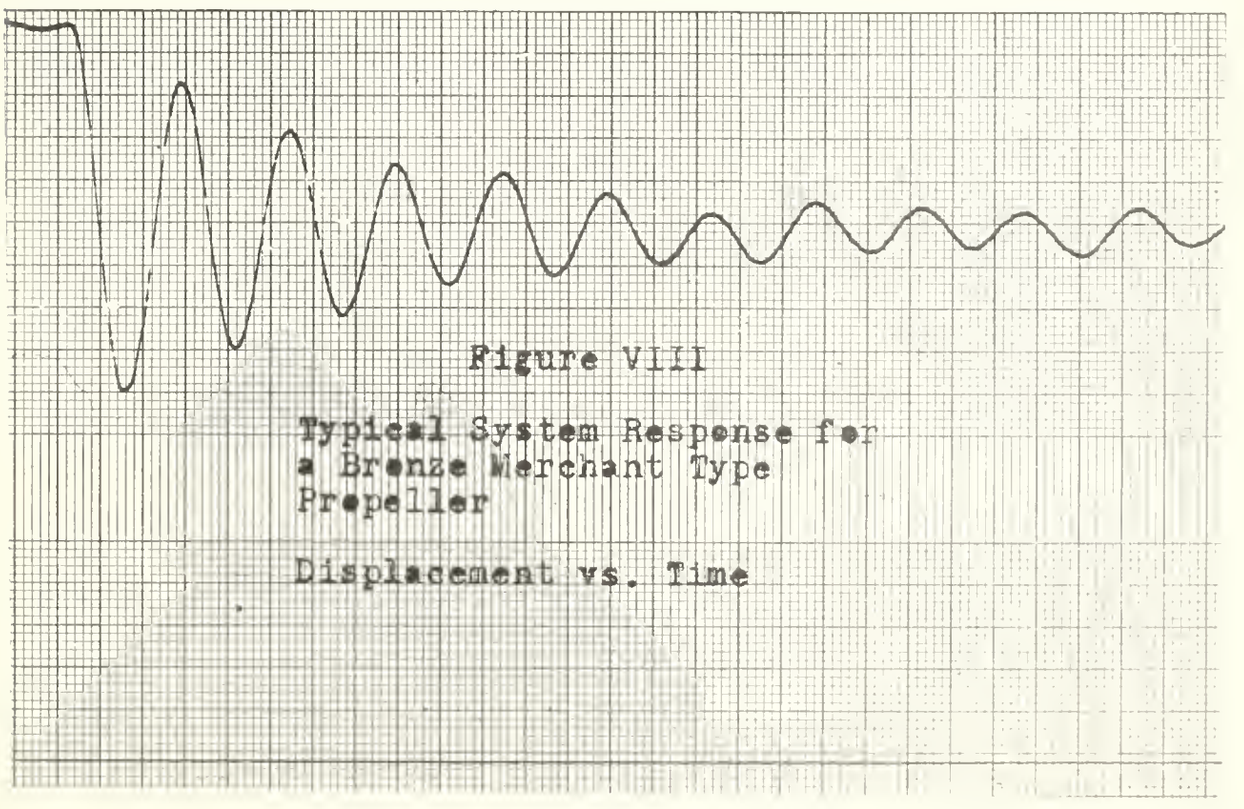

Figure VIII

Typical System Response for a Bronze Merchant Type Propeller

Displacement vs. Time

related to the longitudinal spring constant of the system and to the effective mass of the system. By analyzing the variation of the effective mass between runs in air and in water it was possible to determine the added or virtual mass due to operation in water. The effect of torsional coupling was introduced into the results.

The damping constant is determined by analysis of the exponential decay of the displacement trace. Equation 1 was empirically derived to describe the curve resulting from a plot of virtual mass versus pitch ratio of the propellers.

PROCEDURE

General

The general approach to the measurement was to compare the natural frequency of the vibrating system in water with the natural frequency of the system when in air. The frequency and damping measurements were determined from the transient response of the system following a step displacement from the steady state. These measurements were obtained from the trace of a "Sanborn Recorder, Model 150". The input to the recorder was a half-bridge SR-4 strain gage transducer which was attached to one of the vertical rods which constitute the primary longitudinal spring system.

Method of Excitation

The system was excited by manually displacing the support system longitudinally from its steady state position. This was accomplished by pulling on a piano wire which was connected to the support system through a system of fairleads (Figures I and II). When the piano wire was released suddenly, the system response was an exponentially decaying sinusoid. Caution was taken to ensure that after release no tension existed on the tripping wire. The longitudinal displacement prior to release was approximately 1/8 inch.

Method of Measurement

Figures VII and VIII show a typical response. The period is determined by measurement of the first several cycles of the decaying sinusoid. The first cycle was omitted from this measurement. The exact number of cycles measured depended upon the rate of damping and upon the "noise

level" of the system. This number varied from two to five for runs with the propellers installed. The average number of cycles used was four. The inverse time constant of the exponential decay (α) was determined by use of transparent overlays. Since the damping ratio ($\alpha/\omega_n = \alpha T_o/2\pi$) was always less than .1, no correction was necessary to the damped period in order to obtain the natural period.

The data tabulated for each "Run" represents the arithmetic average of the data obtained from no less than five excitations under the same operating conditions. The excitations for a given "Run" were made within approximately fifteen seconds.

Calibration of the Support System

The propeller supporting system was calibrated in air by adding known weights to the system in lieu of the propeller. The square of the period thus observed (Table I) was then plotted against the weight added (Figure IX). The straight line thus described was then a measure of the longitudinal stiffness of the spring system. i.e. $\Delta W/\Delta T_o^2 = S = 4\pi^2 g/4\pi^2$. Furthermore the extrapolation of this line back to zero period (Figure IX) then measures the weight of the supporting system in air. This weight was found to be 4.89#.

Each time the system was installed in the tunnel the calibration was checked by observing the period of the system with an added weight of 6.562#. The ratio of apparent weight to period squared ($W_a/T_o^2 = S$) was then calculated (W_a being 4.89# + 6.562#). This value of S was then used for the runs made during that day. The slope was checked in the same manner at the conclusion of the day's runs.

level" of the system. This number varied from two to five for runs with the propellers installed. The average number of cycles used was four. The inverse time constant of the exponential decay (α) was determined by use of transparent overlays. Since the damping ratio ($\alpha/\omega_n = \alpha T_o/2\pi$) was always less than .1, no correction was necessary to the damped period in order to obtain the natural period.

The data tabulated for each "Run" represents the arithmetic average of the data obtained from no less than five excitations under the same operating conditions. The excitations for a given "Run" were made within approximately fifteen seconds.

Calibration of the Support System

The propeller supporting system was calibrated in air by adding known weights to the system in lieu of the propeller. The square of the period thus observed (Table I) was then plotted against the weight added (Figure IX). The straight line thus described was then a measure of the longitudinal stiffness of the spring system. i.e. $\Delta W/\Delta T_o^2 = S = 4\pi^2 g/4\pi^2$. Furthermore the extrapolation of this line back to zero period (Figure IX) then measures the weight of the supporting system in air. This weight was found to be 4.89#.

Each time the system was installed in the tunnel the calibration was checked by observing the period of the system with an added weight of 6.562#. The ratio of apparent weight to period squared ($W_a/T_o^2 = S$) was then calculated (W_a being 4.89# + 6.562#). This value of S was then used for the runs made during that day. The slope was checked in the same manner at the conclusion of the day's runs.

Figure IX

Weight Added and W_a vs. T_o^2

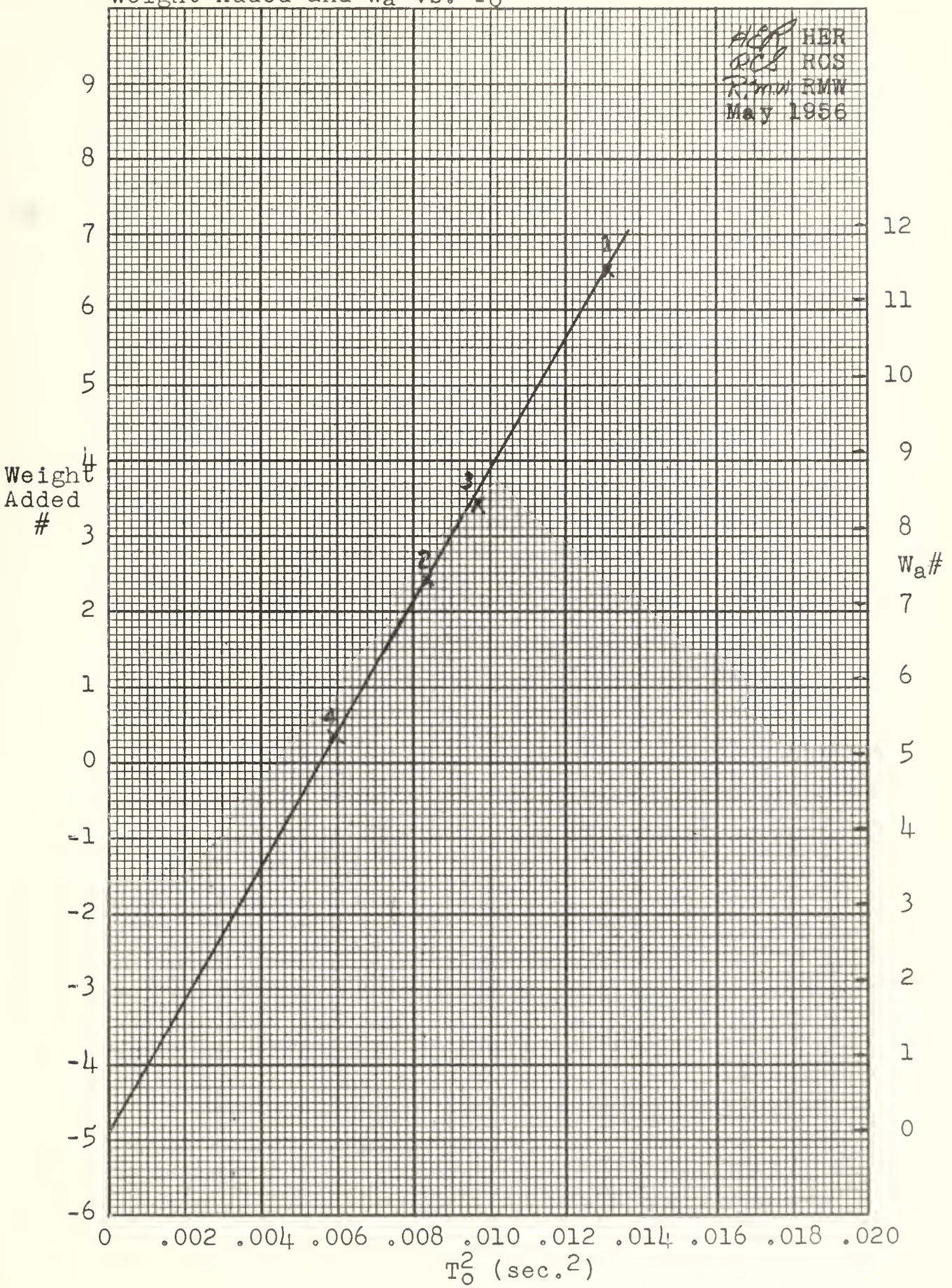

The virtual weight of water and the support damping associated with the oscillation of the support system when immersed in water was determined by use of a dummy hub equal in size to the hub of the merchant type propeller. It was found that for the range of water velocity used in the experiments the virtual weight of the support system was independent of water velocity (see Table II and Figure X). The virtual weight of the water including that actually contained within the bearing support was found to be 0.313#. The virtual weight of the support in water with the merchant type nose and collar piece (W_s) then equals 5.203#. This value was used throughout the merchant type tests. The support damping was found to be dependent upon water velocity and its relationship is plotted in Figure XI.

The virtual weight of water and damping for the support was assumed to be the same for the destroyer type propeller installation. Due to changing the nose pieceand collar for the DD type propeller, the virtual weight of the support in water (W_s) for the DD type propeller is then 4.503#.

Calibration of Recording System

Since the "Sanborn Recorder" used has paper speed errors as great as 1%, it is necessary to correct the measured period for paper speed error. The recorder has a time marker which records one second intervals on one margin of the recording tape (see Figure VII). Since the timing device is an unloaded synchronous motor, the time marker was assumed to have only those errors caused by line frequency variations. The line frequency was monitered and runs were made only when the line frequency was 60cps ± 0.02cps. On this basis corrections were made only for paper speed error.

Figure X
Apparent weight of support in water vs. v_o

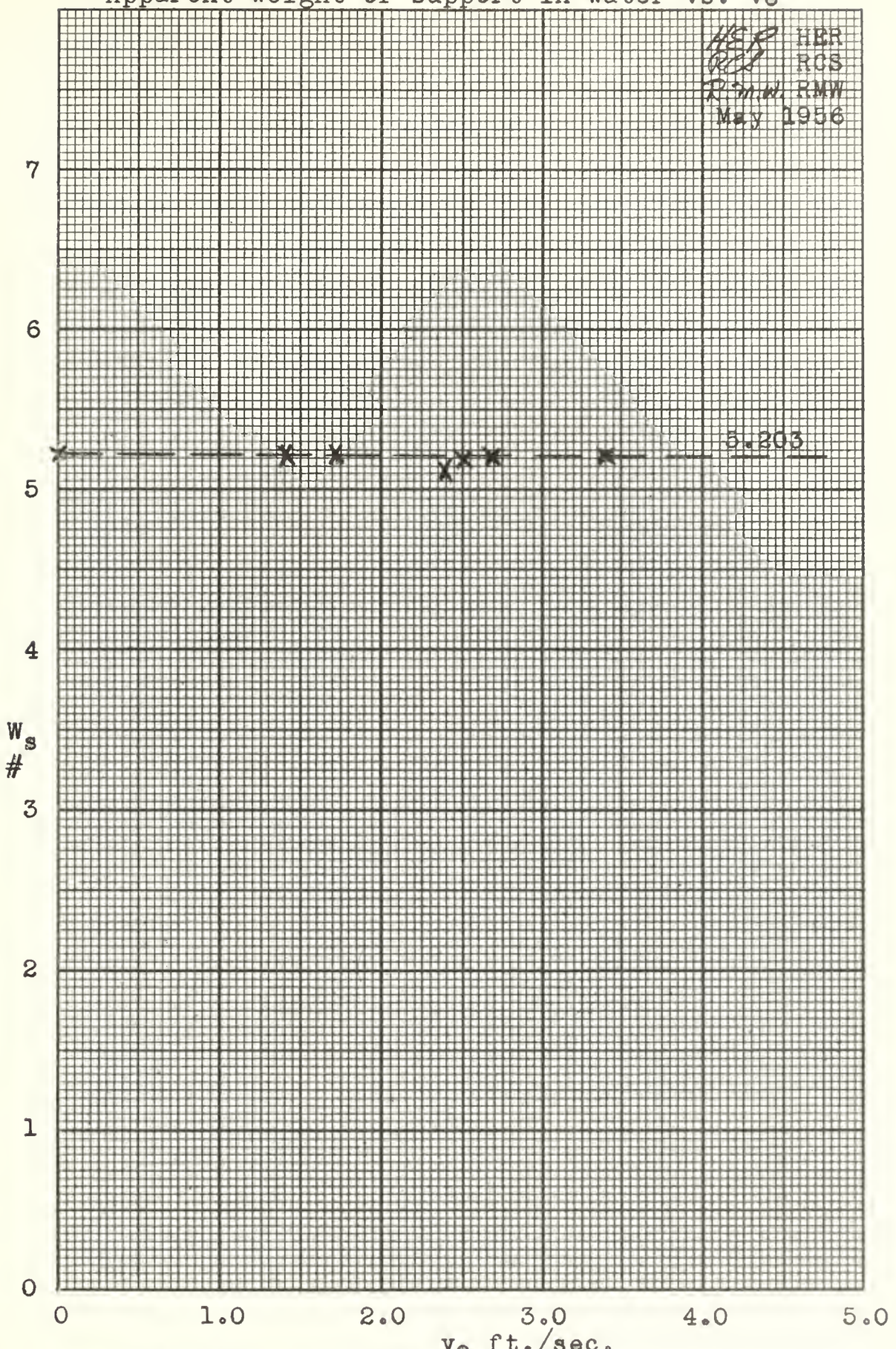

Merchant Type Nose and Hub

Figure XI

Damping Constant for Support vs. Approach Velocity

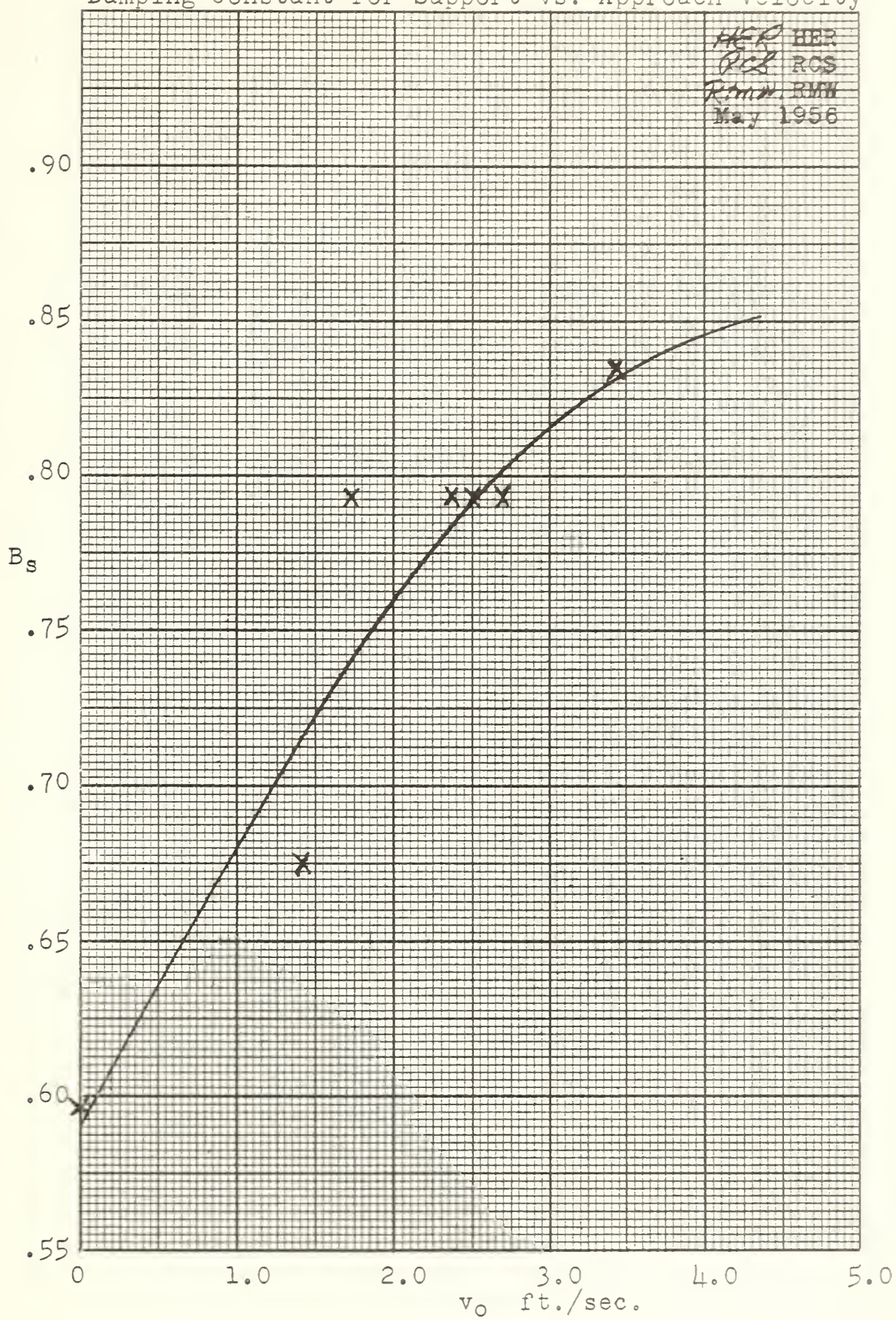

Method of Calculation

The value of T_o which is tabulated in the tables of data was corrected for paper speed error only.

Then: $W_a = S \times T_o^2$

and $W_e = W_a - (W_l + W_s)$

To correct for coupling between torsional oscillation and longitudinal oscillation a torsional coupling factor was determined (see Appendix B).

Then: $W_{a\ corrected} = C_I W_a$

and $W_e' = W_{a\ corrected} - (W_l + W_s)$

The value of α which is tabulated on the tables of data was determined by means of transparent overlays.

Then: $B_a = 2\alpha W_a/g$

and $B_e = B_a - B_s$

The theoretical damping constant (b) was evaluated from the equation (see Appendix B).

$$b = \rho n D^3 \frac{dK_t}{dJ}$$

RESULTS

The data are tabulated in Tables III - XIII of the appendix, each table giving the data pertinent to and the characteristics of a given propeller. Each propeller is identified throughout this paper by its respective MIT number. In Figures XII - XV the number next to a point indicates the experimental run from which the point was determined.

The torsional stiffness of the system (k_θ) for the runs above 200 was 7.34 in#/radian and had a ratio of longitudinal frequency to torsional frequency of 5.1 for the bronze propellers and 4.4 for the aluminum propellers. The runs numbered below 200 had a torsional stiffness k_θ = 86.5 in#/radian and had a ratio of longitudinal frequency to torsional frequency of 1.55 for the bronze propeller and 1.31 for the aluminum propellers. The determination of these ratios was only for the merchant propellers and is more fully covered in the discussion of results section.

Figure XII gives the determination of virtual mass for the merchant propellers in the non-rotating static condition plotted against P/D ratio. The torsional restraint to the propeller was provided by the torsional stiffness of the support and driving system(k_θ) and by the coulomb friction between the system bearings and the system shaft.

The upper curves in Figures XIV and XV give the resultant virtual mass in the non-rotating static condition for destroyer propellers of 3 and 4 blades respectively. All of these runs were taken with the stiff springs of k_θ = 86.5 in#/radian.

Figure XII
W_e vs. P/D (Not corrected)

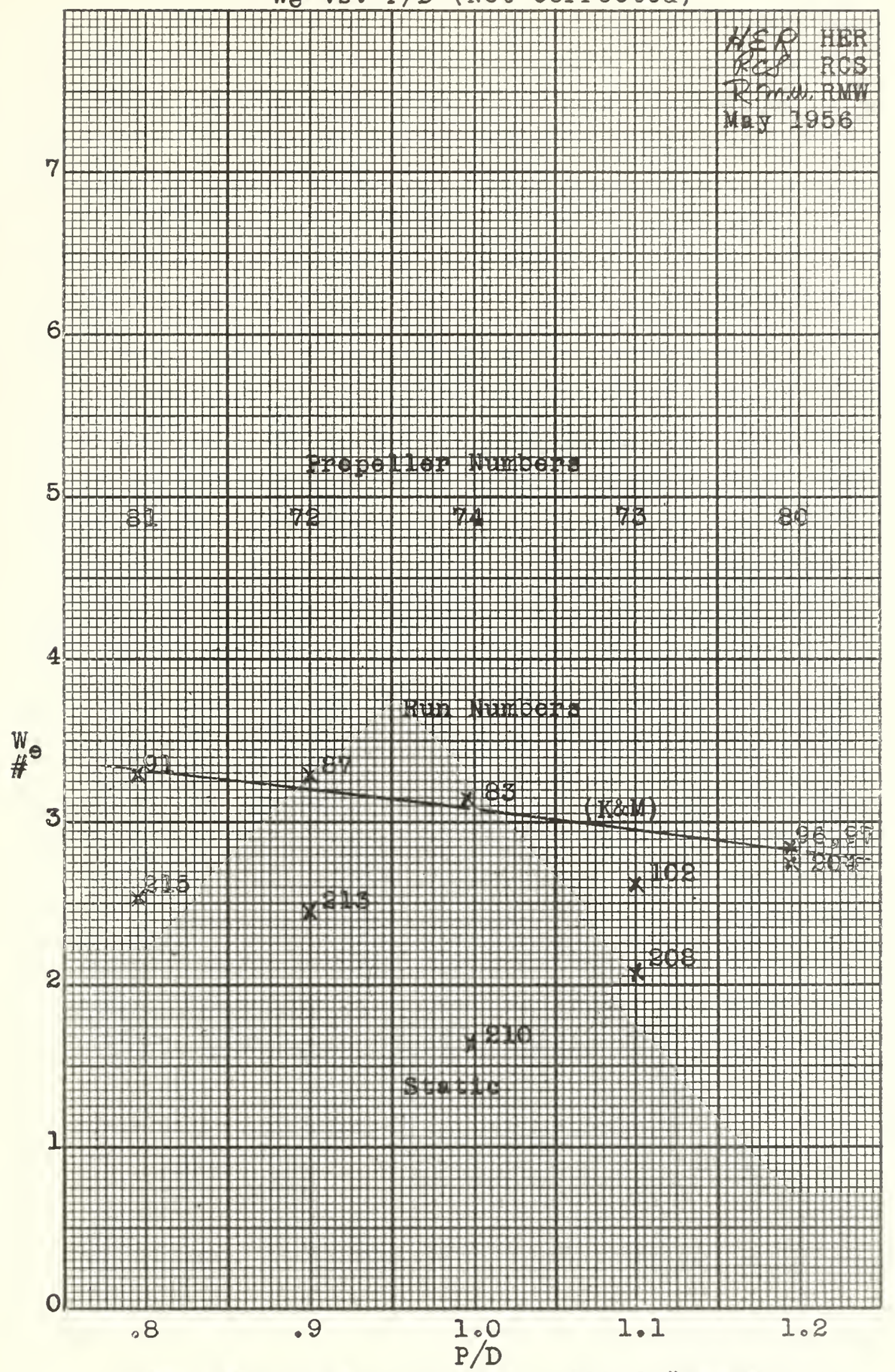

Merchant Type 4 Blades d=11.90" MWR=0.248

Figure XIII
W_e vs. P/D (Not corrected)

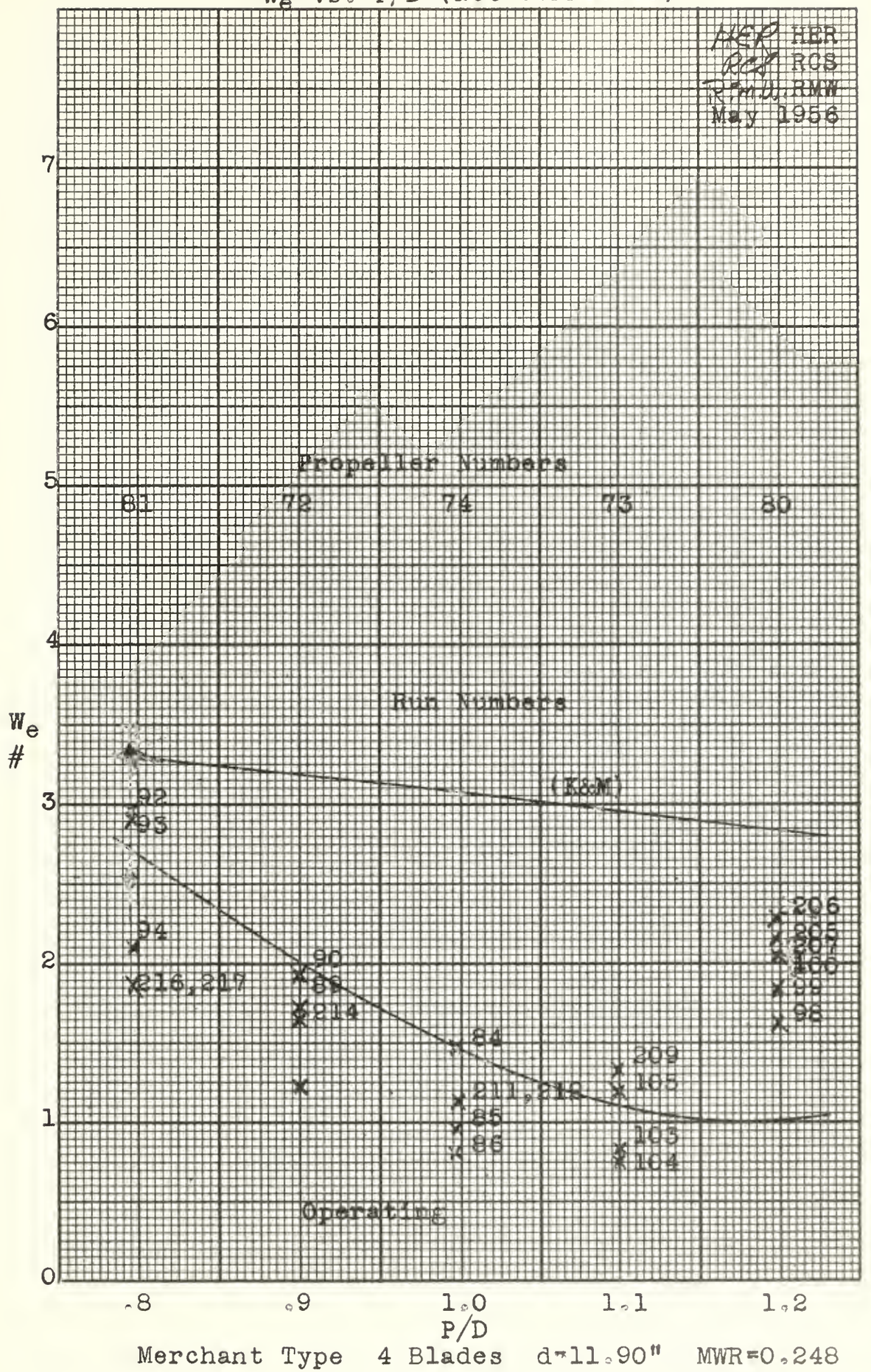

Merchant Type 4 Blades d=11.90" MWR=0.248

Figure XIV
W_e vs. P/D (Not corrected)

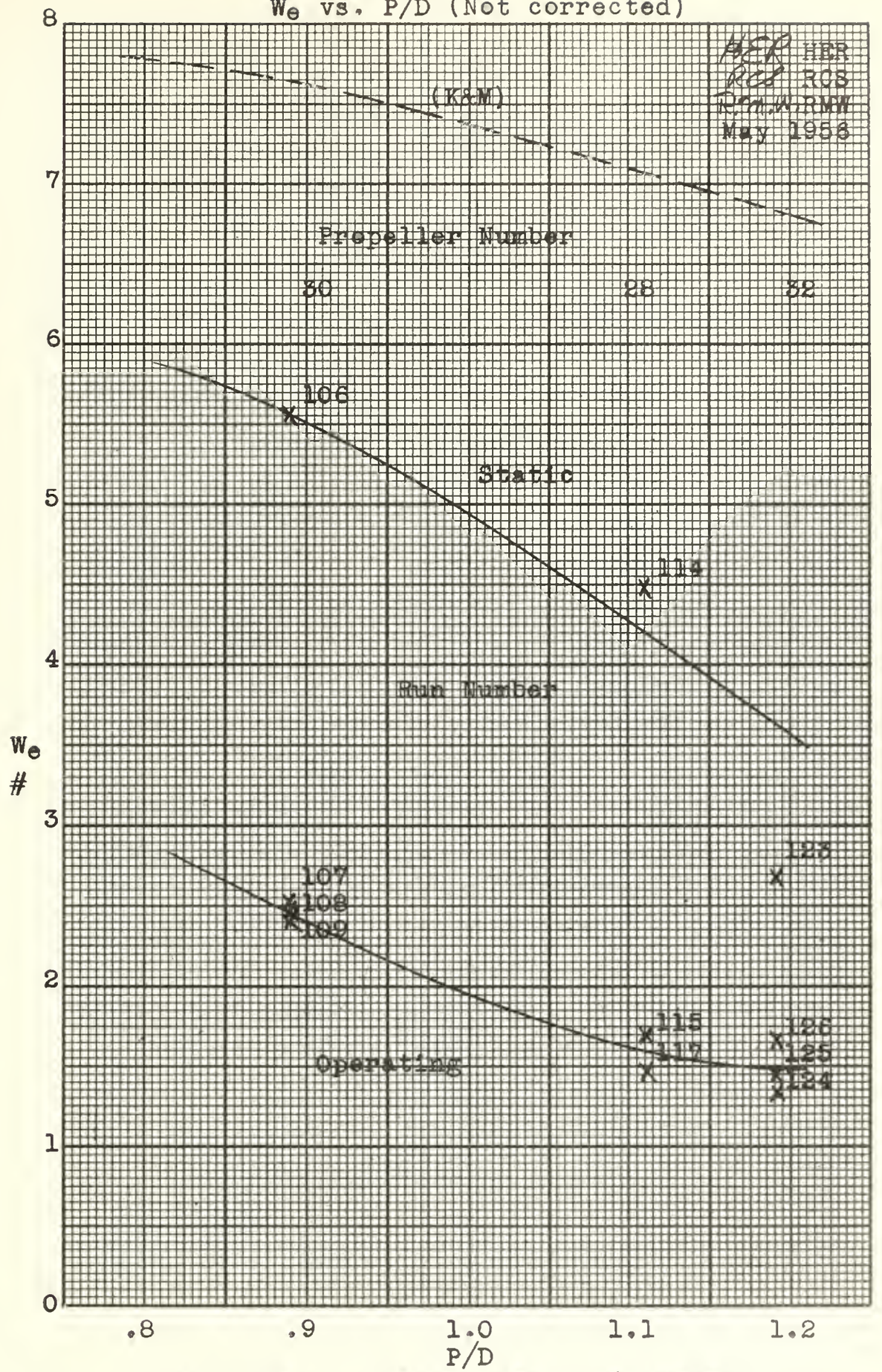

DD409 Type 3 Blades d=11.82" MWR=0.458

Figure XV

W_e vs. P/D (Not corrected)

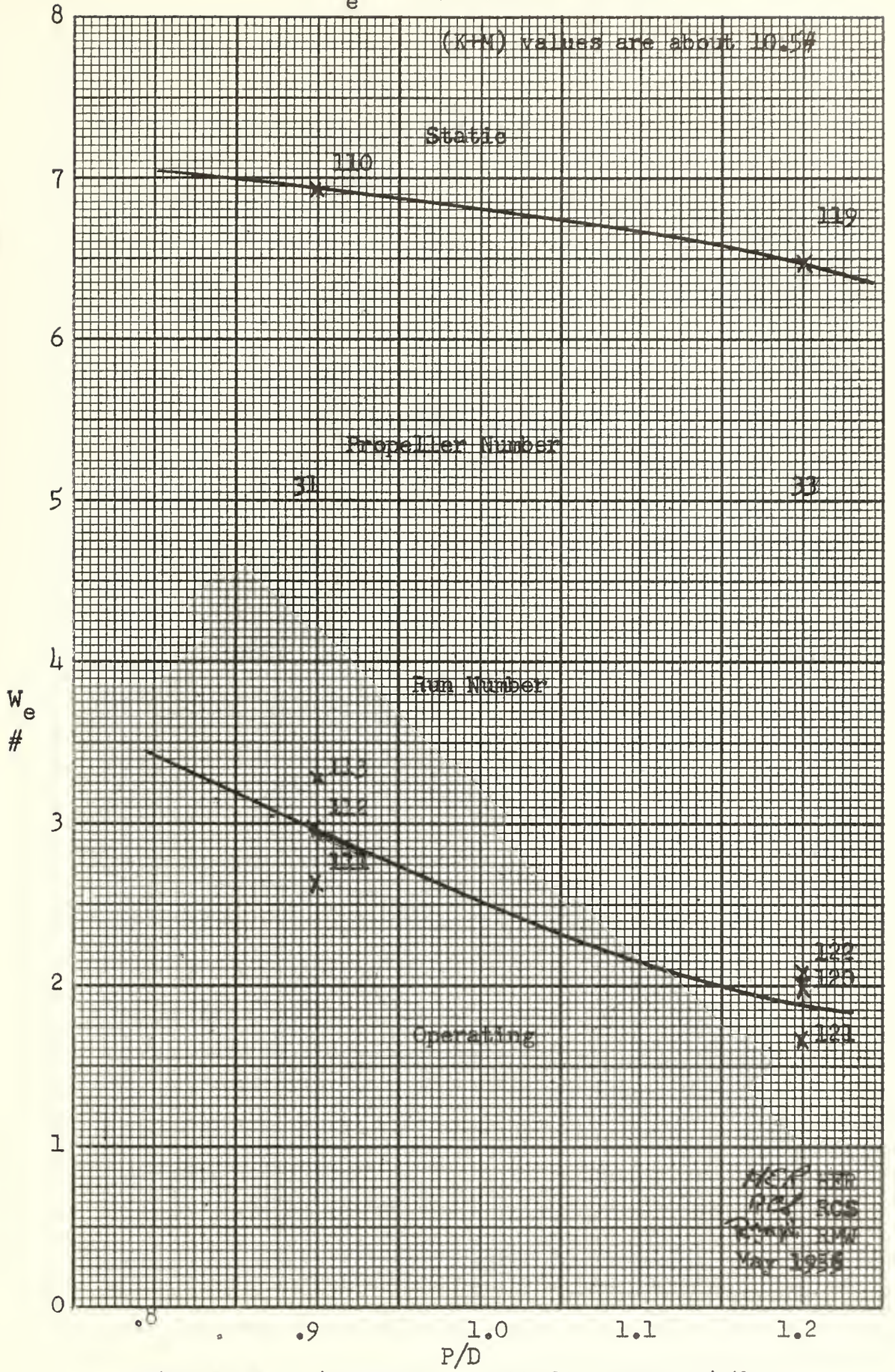

DD409 Type 4 Blades d=11.82" MWR=0.458

Figure XVI
Damping Constant, B_e vs. J

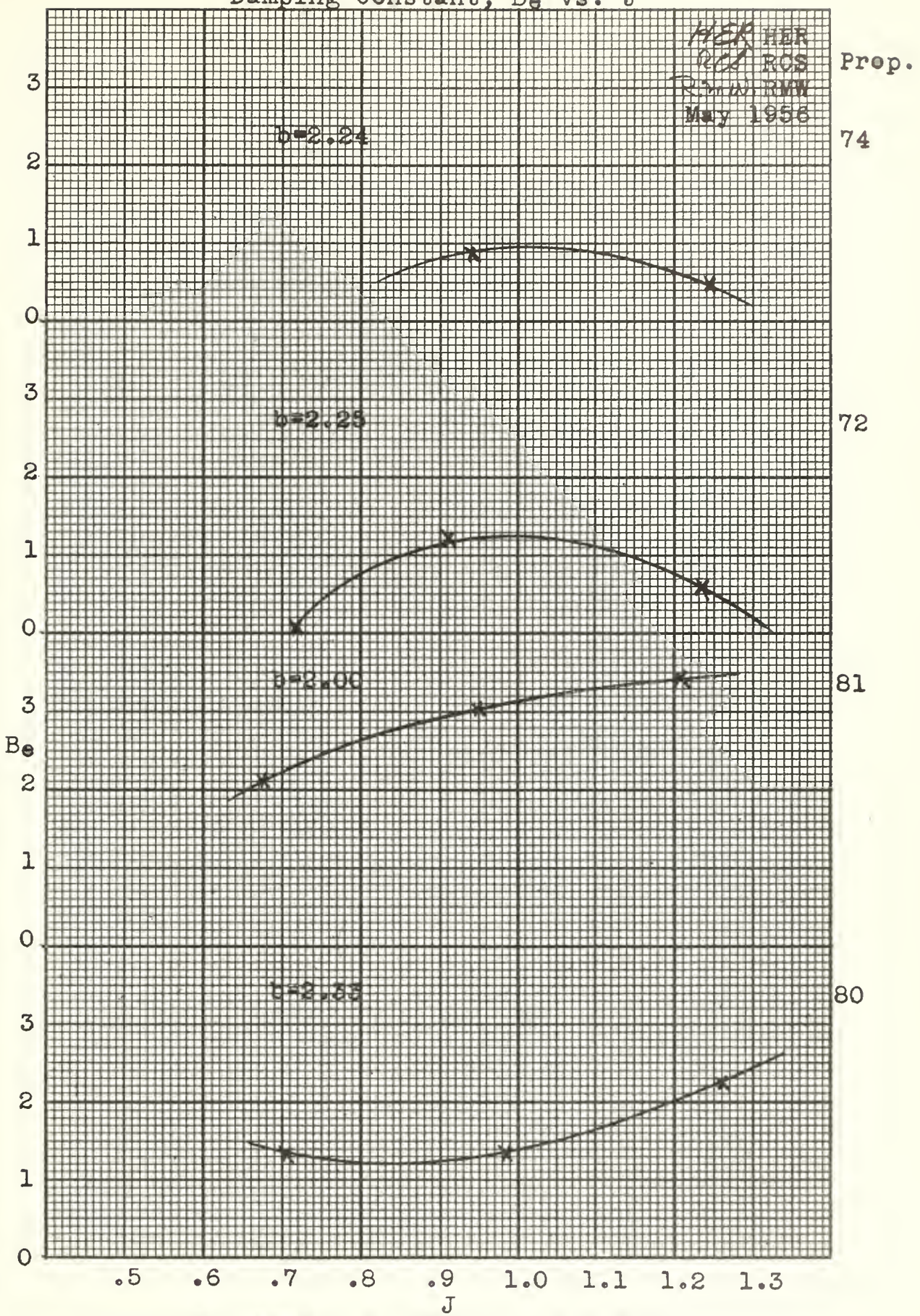

b≡Simple Theoretical Damping Constant

Figure XVII
Damping Constant, Be vs. J

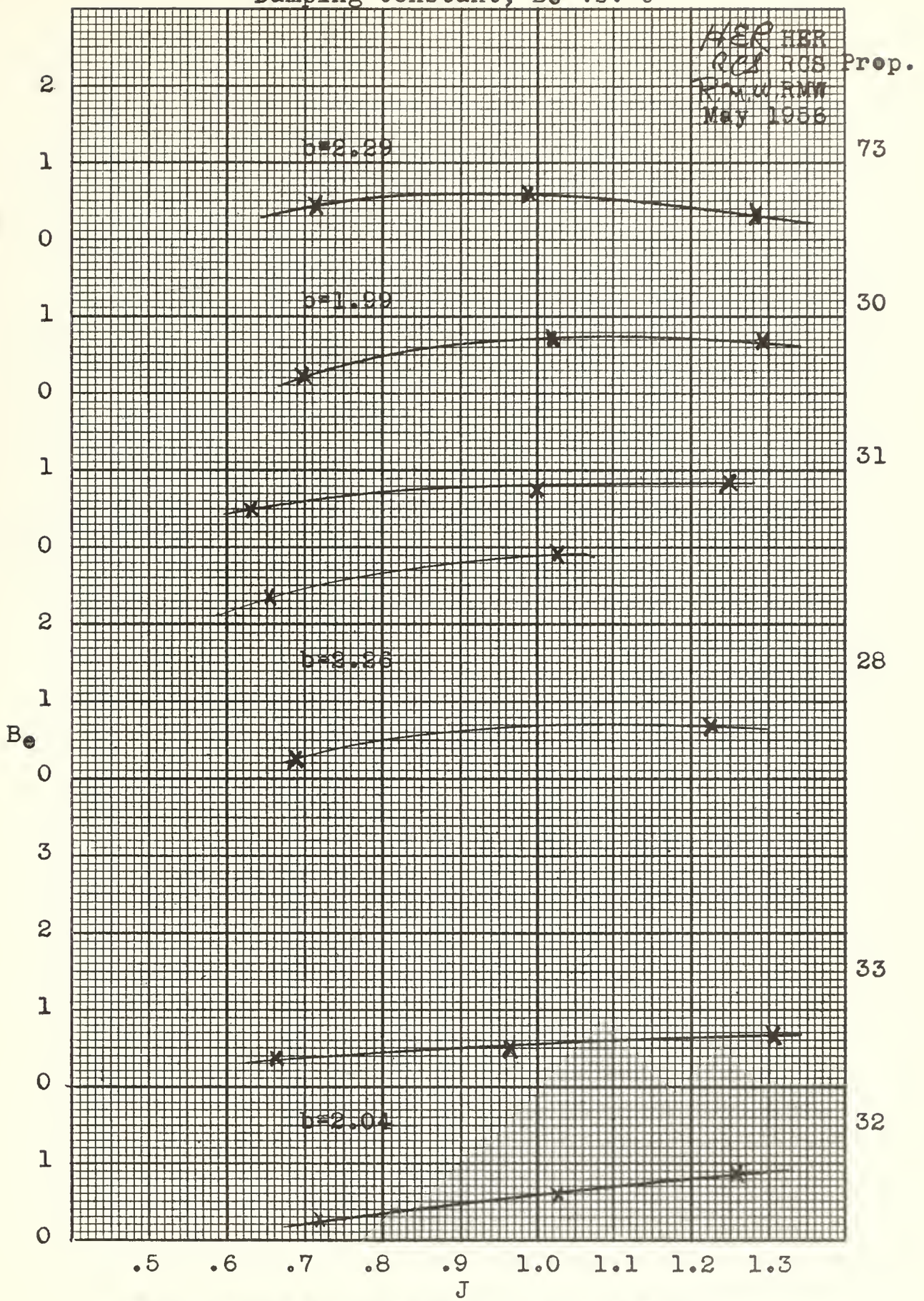

b=Simple Theoretical Damping Constant

Figure XIII gives the virtual mass in the operating condition for the merchant type propellers plotted against P/D ratio.

The lower curves in Figures XIV and XV give the virtual mass in the operating condition for destroyer propellers of three and four blades respectively.

Experimental damping terms (B_e) were calculated from the experimental data and theoretical damping constants (b) were determined from the formulation $b = \rho n d^3 \, dK_t/dJ$ which is derived in appendix B . Both b and B_e are tabulated in Tables III - XIII for all propellers where the necessary data was available. Curves of the experimentally determined B_e which correspond to the theoretically determined values b are drawn in Figures XVI - XVII for each propeller.

DISCUSSION OF RESULTS

Damping

The comparison of the theoretical and experimental values of the damping constant of the propellers in Figures XVI and XVII shows that the experimental values (B_e) are about 30% of the theoretically predicted values (b). The only exception to this was found in propeller number 81 (bronze) which gave a value of B_e which was 25% greater than the predicted value. There was no consistent variation of the damping constant with the speed coefficient ($J = v_o/nd$). More theoretical analysis is recommended.

Virtual weight of water without torsional coupling correction

The virtual weight as determined without the torsional coupling correction is tabulated in Tables III-XIII and is plotted in Figures XII-XV versus P/D ratio. No consistent variation in W_e with speed coefficient (J) was observed for the operating runs.

It is to be noted that the value of W_e determined from the operating runs is much lower than the value determined for the runs with the propeller stopped. For the merchant type propellers the latter values conform very closely to the W_e as predicted by the Kane and McGoldrick formulation (1).

In general the trend of the values of W_e as plotted in Figures XIII-XV is to decrease with increasing P/D. This is the trend which would be anticipated from physical reasoning. If this trend had been entirely consistent, it would have been possible to conclude that our calculated values of W_e were a true representation of the virtual weight. The inconsistency is that the bronze propeller #80 with a

P/D of 1.195 has a value of W_e which is appreciably greater than the value to be expected from a fair curve through the values of W_e determined for the aluminum merchant type propellers having lower P/D ratios.

It is felt that this apparent discrepancy is due to the fact that the polar inertia of the aluminum propeller is less than that of the bronze propeller and is, because of this lower inertia, more subject to torsional coupling than is the bronze propeller.

Before investigating the effect of the lower polar inertia of the aluminum propellers the relationship between the first approximation longitudinal and torsional characteristics of the apparatus were investigated. A variation of the torsional characteristics of the system was achieved by varying the stiffness of the torque transmission springs. The runs numbered above 200 were run with springs of k_e = 7.34 in#/radian and the other runs were with springs giving a k_e = 86.5 in#/radian. Since this torsional stiffness is much lower than that of the drive shaft (k_θ = 2500), a first approximation of the torsional frequency of the system may be arrived at by considering the k_θ of the torque transmission system alone. The longitudinal spring constant k_L has inherently been used to determine the virtual mass and is readily evaluated.

Values of the first approximation torsional frequency and the longitudinal frequency are determined below for one arbitrarily selected bronze propeller and one of aluminum. As illustrated in Figures XII-XV, the shift in the frequency ratios apparently had negligible effect on the amount of torsional coupling. (By comparison of 200 runs and other runs with the same propeller.)

System #2	System #1
Runs Above 200	Runs Below 200
Soft Springs	Stiff Springs
$k_L = 83.4$ #/in, $k_\theta = 7.34 \frac{in\#}{radian}$	$k_L = 89$, $k_\theta = 86.5$
Bronze Propeller #80 Run 205	Run 100
$f_L = \frac{1}{.13485} = 7.42$ /sec	$f_L = \frac{1}{.12920} = 7.75$ /sec
$I_p = (1.25)(.0706) = 0.0884$	$I_p = .0884$
$f_\theta = 1.45$ /sec	$f_\theta = 5.0$ /sec
$f_L/f_\theta = 5.1$	$f_L/f_\theta = 1.6$
Aluminum Propeller #74 Run 211	Run 85
$f_L = \frac{1}{.1033} = 9.66$ /sec	$f_L = \frac{1}{.1010} = 9.9$ /sec
$I_p' = (.287 + .25).0706 = 0.038$	$f_\theta = 7.56$ /sec
$f_\theta = 2.21$ /sec	$f_L/f_\theta = 1.31$
$f_L/f_\theta = 4.4$	

Torsional Coupling

To make allowance for the variation in polar inertia between the aluminum and the bronze propellers and to obtain an "absolute" value of virtual mass, torsional coupling was investigated and a torsional coupling factor was derived. The "absolute" value of virtual mass is defined as the value which would have been observed if there had been

no torsional coupling.

Torsional coupling is a measure of the interaction of torsional and longitudinal vibrations. The greater the torsional coupling the less will be the amount of water entrained longitudinally by the rotating propeller.

Applying this to the experiments conducted it may be seen that if either the polar moment of inertia of the propeller or the torsional stiffness of the driving shaft (or coupling) is low, the amount of torsional coupling will be large.

In the shipboard case (4) little torsional coupling should be expected. In our determination the polar moment of inertia and the torsional spring constant are low so that some torsional coupling is anticipated. Therefore a torsional coupling factor, C_I, was derived by assuming that the experimental determination corresponded to a case of high torsional coupling and that a correction to the condition of low torsional coupling was necessary. (i.e. $k_\theta = \infty$).

The basis for this torsional coupling correction is an unpublished paper by Professor Frank M. Lewis of the Massachusetts Institute of Technology. (See extract in Appendix C).

The derivation of C_I and sample calculations are detailed in Appendix B. The values of C_I varied from 1.02 for a bronze propeller to 1.11 for an aluminum propeller. This correction was applied to the system weight W_a and led to a corrected virtual weight of entrained water W_e', recorded in Tables III-XIII and in Figures XVIII-XX.

Errors in the Measurement

The major source of error in the measurement was in the assumption

that the longitudinal stiffness of the system was constant during the runs made on a given day. The stiffness was found to vary by a maximum of about 2% from the initial determination made prior to the runs to the final determination made after the runs. The reason for this variation is unknown.

The measurement of the period (T_o) by the method outlined in the Procedure is estimated to be accurate to within 1%.

The paper speed correction and the variation line of frequency are each estimated to be accurate to within 0.1%.

The above errors then give an estimated error of 3.2% in the determination of the observed period (T_o). This corresponds to an error of 6.4% in T_o^2 and in W_a. The mean value of W_a (aluminum) is about 9# and the mean value of W_a (bronze) is about 15# for the merchant type propellers. The mean value of W_a for the DD type propellers is about 9#.

This then corresponds to an estimated total error of .57# in the determination of W_e(and/or W_e') for the aluminum merchant type propellers and for the DD type propellers. The total error in the bronze merchant type propellers is then .96#. This estimate of the error of the measurement is confirmed very well by Figures XIII-XV.

Concluding Discussion

On the basis of the virtual mass corrected for torsional coupling an empirical relationship was derived to describe the variation of virtual mass with the important parameters. The derivation is given in Appendix B and leads to the following:

$$W_e'_{(rsw)} = 5.773\left[\left(1.350 - (P/D)\right)^2 + 0.228\right] \left(\frac{d}{10}\right)^3 N^{0.8} MWR^{1.13} \quad (1)$$

Figure XVIII

W'_e (average, corrected) vs. P/D

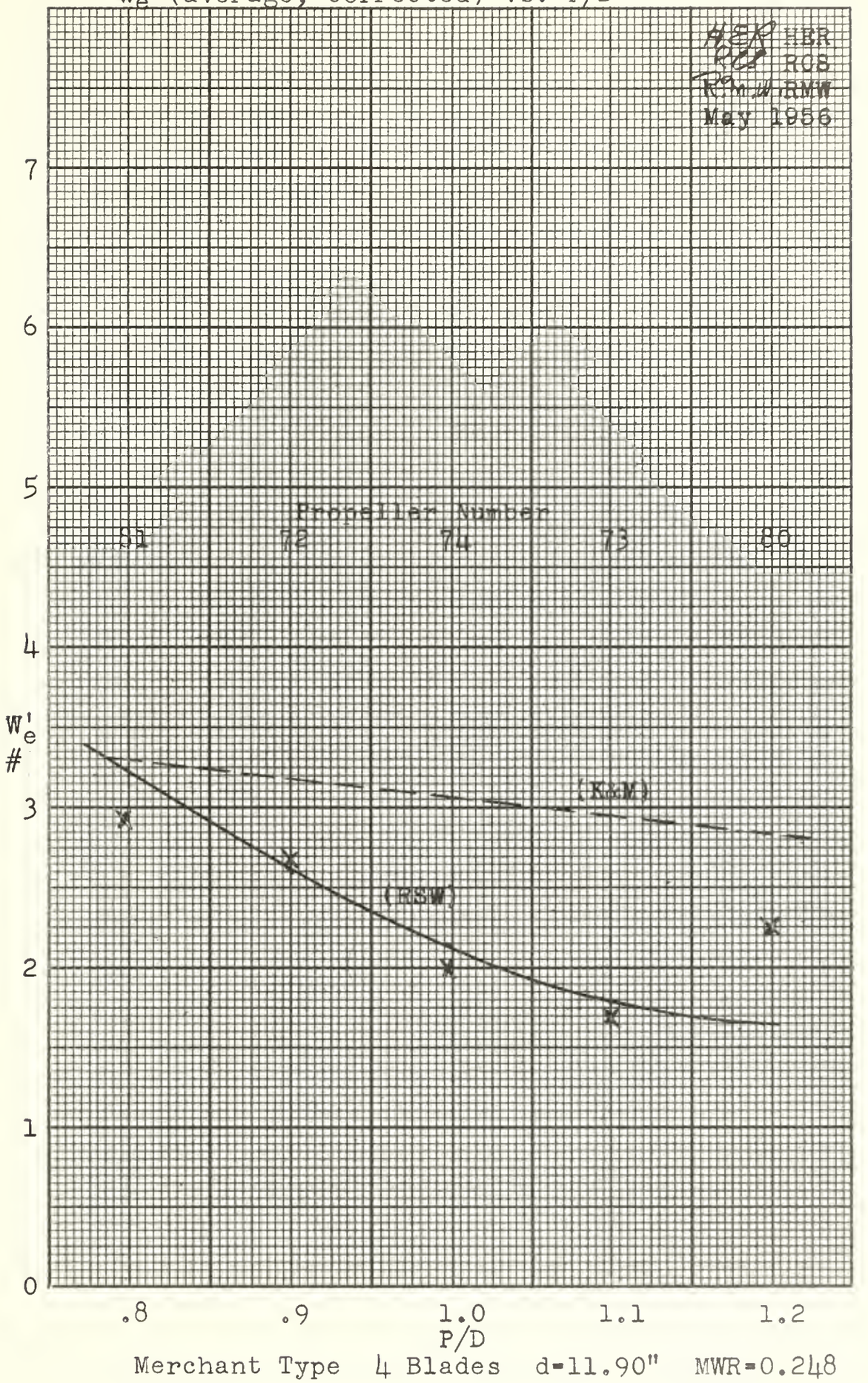

Merchant Type 4 Blades d=11.90" MWR=0.248

Figure XIX

W_e' (average, corrected) vs. P/D

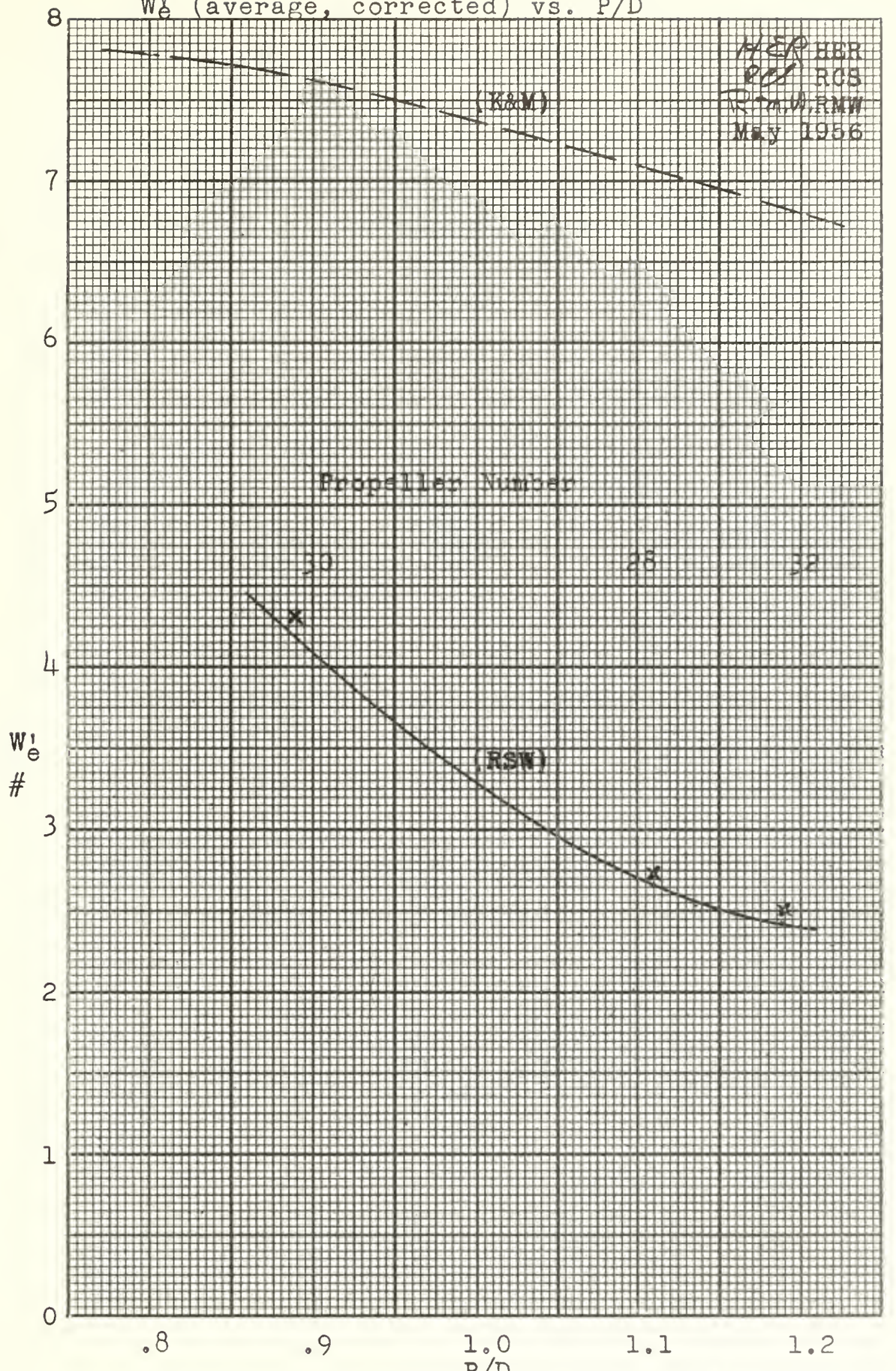

DD409 Type 3 Blades d=11.82" MWR=0.458

Figure XX

W'_e (average, corrected) vs. P/D

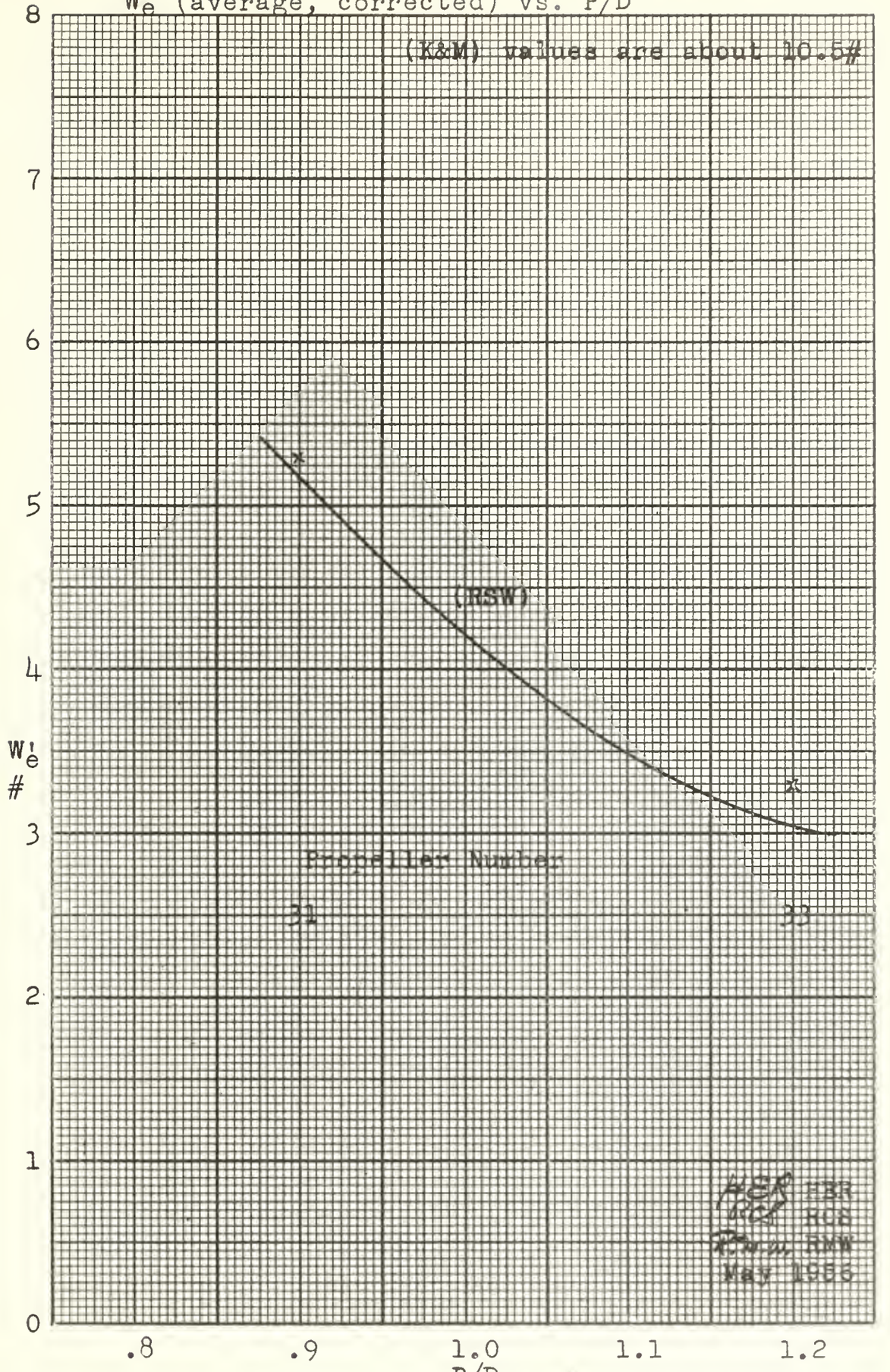

DD409 Type 4 Blades d=11.82" MWR=0.458

This equation held for both the low mean width ratio (.248) merchant propellers and the high (.458) MWR destroyer propellers. It gives the absolute virtual mass, that is the virtual mass with no torsional coupling. This corresponds to the shipboard case where torsional coupling is not anticipated. The values of W_e, W_e', $W_{e'(rsw)}$, and $W_{e(K\&M)}$ are tabulated in Table IA. It is our conclusion that $W_{e'(rsw)}$ gives a quick and sufficiently accurate determination for use in shipboard calculations.

To improve on our determination, more analysis of the effect of torsional spring and inertia coupling is required. The manufacture of two propellers, one bronze and one aluminum, of the same characteristics would allow comprehensive testing and absolute determination of the variation in longitudinal virtual mass due solely to variation in the polar inertia of the propeller. Also, propellers of varying diameter should be tested to determine the diameter influence and to compare it with the theoretical prediction of variation of virtual mass with the cube power of the diameter.

TABLE IA

Comparison of virtual weight of entrained water as determined by various methods.

Prop. No.	W_B wt of prop corrected to Bronze	P/D	W_e	W_e'	W_e'(rsw)	$W_{e(K\&M)}$
81	7.44	.796	2.65	2.94	3.26	3.3
72	7.85	.90	1.57	2.68	2.63	3.2
74	7.85	.9975	1.07	1.99	2.15	3.07
73	7.65	1.099	.87	1.70	1.77	2.95
80	7.47	1.195	1.83	2.25	1.47	2.84
30	10.0	.890	2.48	4.31	4.18	7.65
28	10.0	1.11	1.46	2.72	2.67	7.05
32	10.0	1.19	1.51	2.50	2.41	6.80
31	11.3	.90	2.98	5.30	5.16	10.7
33	11.3	1.20	1.92	3.26	3.00	9.5

(1) $$W_e'(rsw) = 5.775 \left[(1.350-P/D)^2 + .228\right] \left(\frac{d}{10}\right)^3 (N^{.8})\, MWR^{1.13}$$

$$W_{e(K\&M)} = 9100 \times \frac{1}{.23\left(\frac{P}{d}\right)^2 + 1} \times N \times \left(\frac{d}{100}\right)^3 (MWR)^2$$

where: W_e is the experimentally observed value

W_e' is the observed value corrected to condition of infinite torsional stiffness of coupling

W_e'(rsw) is the value predicted by equation

W_e (K&M) is the value predicted by the Kane and McGoldrick formulation (1)

CONCLUSIONS

1. Virtual weight of entrained water can be expressed by the following equation:

$$W_{e'(rsw)} = 5.775 \left[(1.350-P/D)^2 + .228\right]\left[\left(\frac{d}{10}\right)^3\right]\left[N^{.8}\right]\left[MWR^{1.13}\right] \text{ lbs.}$$

$0.75 < P/D < 1.25$

P/D = Pitch ratio

d = Propeller diameter (in)

N = Number of blades

MWR = Mean width ratio

2. The following percentages represent the virtual weight for a sampling of bronze propellers on the basis of total weight of propeller blades: (blade thickness fraction = 0.05)

P/D	4 Bladed Merchant	3 Bladed DD	4 Bladed DD
.9	71%	71%	72%
1.2	44%	41%	42%

3. The values of virtual weight under actual operating conditions were significantly less than the values predicted on the basis of non-rotating static tests. This was particularly true for the DD types.

4. There was no consistent variation of virtual weight with variation of J in the operating range.

5. Magnitudes of damping factors under operating conditions were about 30% of the theoretically predicted values. There were no significant trends with a variation of J or v_o.

RECOMMENDATIONS

1. Investigate torsional coupling factor to a greater degree, particularly the effect of varying polar moment of inertia. It would be advantageous to compare aluminum and bronze propellers having the same geometrical characteristics.

2. Obtain data for more propellers to establish curves more thoroughly. To determine or prove scaling factor run geometrically similar propellers of varying diameters.

3. Investigate damping more thoroughly varying the parameters.

4. Investigate the variation of longitudinal stiffness of the support.

APPENDIX

A. Summary of Data and Calculations

TABLE I

CALIBRATION OF SUPPORT SYSTEM IN AIR

RUN	Wt added	T_o	T_o^2
1	6.562	.1142	.01320
2	2.469	.0919	.00844
3	3.469	.0993	.00986
4	0.375	.0775	.00600

The weight of the supporting system in air including the nose and collar used with the merchant type propellers was determined to be 4.89#. This was determined by extrapolating the curve of weight added versus T_o^2 to the value of T_o^2 equals zero. (See figure IX).

TABLE II

CALIBRATION OF SUPPORT SYSTEM IN WATER

Added weights---Dummy hub wt = .812#

Water in hub = .375#

Wt added = 1.187#

RUN	N	h	v_o	T_o	T_o^2	W	W_s	α	B_s
1	0	0	0	.08835	.007795	6.43	5.243	1.5	.595
2	0	32.9	2.39	.08740	.007640	6.30	5.113	2.0	.799
3	0	35.9	2.50	.08795	.007735	6.38	5.193	2.0	.794
4	0	11.4	1.41	.08820	.007780	6.42	5.233	1.7	.675
5	0	17.0	1.72	.08805	.007750	6.40	5.231	2.0	.794
6	0	41.6	2.69	.08735	.007630	6.30	5.221	2.0	.794
7	0	66.4	3.40	.08725	.007610	6.28	5.219	2.1	.834

$W_s = W - 1.187\#$

TABLE III

M.I.T. PROPELLER NO. 81

Merchant Type

Material = Bronze

Diameter (d) = 11.90"

No. of Blades (N) = 4

Pitch Ratio (P/D) = 0.796

Mean Width Ratio (MWR) = 0.248

dK_t/dJ $.4 < J < .9$ = .452

S = 836 (Runs 91 - 94); 815 (Runs 215 - 217)

W_p = 7.437#

W_h = 0

W_l = 7.437#

W_s = 5.203#

RUN	h	t	v_o	N	J	T_o	T_o^2	W_a	W_e	α	B_a	B_s	B_e	b
91	0	-	0	0	-	.1380	.01903	15.910	3.27	0.8	.99	.59	0.40	
92	17.0	69.5	1.72	151	.68	.1364	.01861	15.560	2.92	3.0	2.85	.74	2.11	2.15
93	33.5	69.5	2.91	152	.95	.1366	.01865	15.590	2.95	4.0	3.80	.79	3.01	2.17
94	60.0	69.5	3.23	160	1.21	.1327	.01761	14.730	2.09	4.5	4.28	.82	3.46	2.28
215	0	-	0	0	-	.1364	.0186	15.15	2.51					
216	31.5	70	2.34	143	.98	.1333	.01775	14.50	1.86					
217	25	70	2.08	144	.87	.1333	.01775	14.50	1.86					

Run 217 readings of T_o were erratic.

W_a (average, operating) = 14.976#

W_e' = 2.94#

TABLE IV

M.I.T. PROPELLER NO. 72

Merchant Type

Material = Aluminum

Diameter (d) = 11.90"

No. of Blades (N) = 4

Pitch Ratio (P/D) = 0.900

Mean Width Ratio (MWR) = 0.248

dK_t/dJ $.5 < J < 1.1$ = .465

S = 836 (Runs 87 - 90); 815 (Runs 213, 214)

W_p = 2.250#

W_h = 0.063#

W_l = 2.313#

W_s = 5.203#

RUN	h	t	v_o	N	J	T_o	T_o^2	W_a	W_e	α	B_a	B_s	B_e	b
87	0	-	0	0	-	.1137	.01292	10.80	3.284	1.6	1.07	.59	0.48	
88	18.6	69.5	1.79	151	.71	.1022	.01044	8.73	1.214	1.5	0.85	.75	0.10	2.21
89	30.3	69.5	2.29	152	.91	.1050	.01103	9.22	1.704	3.5	1.98	.78	1.20	2.23
90	59.0	69.5	3.20	156	1.23	.1056	.01115	9.32	1.904	2.5	1.41	.82	0.59	2.29
213	0	-	0	0	-	.1111	.01234	10.06	2.44					
214	40	70	2.64	140	1.13	.1060	.01123	9.16	1.64					

W_a (average, operating) = 9.107#

W_e' = 2.68#

TABLE V

M.I.T. PROPELLER NO. 74

Merchant Type

Material = Aluminum

Diameter (d) = 11.90"

No. of Blades (N) = 4

Pitch Ratio (P/D) = 0.9975

Mean Width Ratio (MWR) = 0.248

dK_t/dJ $.5 < J < 1.2$ = .472

S = 836 (Runs 83 - 86); 815 (Runs 210 - 212)

W_p = 2.250#

W_h = 0.125#

W_1 = 2.375#

W_s = 5.203#

RUN	h	t	v_o	N	J	T_o	T_o^2	W_a	W_e	α	B_a	B_s	B_e	b
83	0	-	0	0	-	.1133	.01284	10.73	3.152	1.8	1.20	0.59	0.61	
84	32.0	68.0	2.36	150	.94	.1041	.01083	9.05	1.472	3.1	1.66	0.78	0.88	2.23
85	57.3	68.0	3.16	152.5	1.24	.1010	.0102	8.53	.952	2.4	1.29	0.82	0.47	2.27
86	16.9	68.0	1.714	150	.68	.1001	.01002	8.38	.802	1.2	0.64	0.73	0.09	2.23
210	0	-	0	0	-	.1063	.01130	9.21	1.63					
211	36	70	2.50	148	1.01	.1035	.010712	8.74	1.16					
212	47.5	70	2.88	142	1.21	.1031	.010630	8.67	1.09					

W_a (average, operating) = 8.674#

W_e' = 1.99#

TABLE VI

M.I.T. PROPELLER NO. 73

Merchant Type

Material = Aluminum

Diameter (d) = 11.90"

No. of Blades (N) = 4

Pitch Ratio (P/D) = 1.099

Mean Width Ratio (MWR) = 0.248

dK_t/dJ $.65 < J < 1.2$ = .472

S = 881 (Runs 102 - 105); 815 (Runs 208, 209)

W_p = 2.219#

W_h = 0.125#

W_l = 2.334#

W_s = 5.203#

RUN	h	t	v_o	N	J	T_o	T_o^2	W_a	W_e	α	B_a	B_s	B_e	b
102	0	-	0	0	-	.1074	.01154	10.16	2.623	1.7	1.07	.59	.48	
103	19.5	67.5	1.84	154	.72	.09706	.00942	8.30	0.773	2.3	1.17	.75	.42	2.29
104	38.0	67.5	2.57	156	.99	.09668	.00935	8.24	0.713	2.7	1.40	.80	.60	2.32
105	61.0	67.5	3.26	152	1.28	.09938	.00988	8.70	1.173	2.2	1.15	.83	.32	2.26
208	0	-	0	0	-	.1085	.01177	9.59	2.05					
209	45	68	2.79	150	1.12	.1040	.01082	8.82	1.28					

W_a (average, operating) = 8.515#

W_e' = 1.70#

TABLE VII

M.I.T. PROPELLER NO. 80

Merchant Type

Material = Bronze

Diameter (d) = 11.90"

No. of Blades (N) = 4

Pitch Ratio (P/D) = 1.195

Mean Width Ratio (MWR) = 0.248

dK_t/dJ $.7 < J < 1.3$ = .494

S = 881 (Runs 96 - 100); 815 (Runs 204 - 207)

W_p = 7.470#

W_h = 0

W_l = 7.470#

W_s = 5.203#

RUN	h	t	v_o	N	J	T_o	T_o^2	W_a	W_e	α	B_a	B_s	B_e	b
96	0	-	0	0	-	.1349	.01761	15.51	2.837	-	-	-	-	
97	0	-	0	0	-	.13045				0.8	0.77	.59	.18	
98	18.0	67	1.77	150	.708	.12728	.01621	14.30	1.627	2.3	2.07	.74	1.33	2.33
99	35.0	67	2.46	150	.985	.12828	.01646	14.51	1.837	2.4	2.12	.79	1.33	2.33
100	57.5	67	3.16	150	1.264	.12920	.01669	14.71	2.047	3.4	3.10	.82	2.28	2.33
204	0	-	0	0	-	.1375	.01890	15.41	2.74					
205	59	68	3.20	154	1.25	.13485	.01818	14.81	2.14					
206	57	68	3.15	152	1.24	.1352	.01828	14.90	2.23					
207	41	68	2.67	105	1.53	.1343	.01805	14.71	2.04					

W_a (average, operating) $= \frac{87.94}{6} = 14.656\#$

$W_e' = 2.25\#$

TABLE VIII

M.I.T. PROPELLER NO. 30

DD409

Material = Aluminum

Diameter (d) = 11.82"

No. of Blades (N) = 3

Pitch Ratio (P/D) = 0.890

Mean Width Ratio (MWR) = 0.458

dK_t/dJ $.4 < J < .93$ = .427

S = 881

W_p = 2.875#

W_h = 0.063#

W_1 = 2.938#

W_s = 4.503#

RUN	h	t	v_o	N	J	T_o	T_o^2	W_a	W_e	α	B_a	B_s	B_e	b
106	0	-	0	0	-	.12136	.01472	13.00	5.56	1.52	1.23	.59	.64	
107	18.0	67.5	1.77	152	.70	.10630	.01130	9.96	2.52	1.55	.95	.74	.21	2.00
108	37.5	67.5	2.55	150	1.02	.10610	.01126	9.94	2.50	2.42	1.49	.79	.70	1.98
109	60.0	67.5	3.23	150	1.29	.10590	.01122	9.90	2.46	2.45	1.51	.82	.69	1.98

W_a (average, operating) = 9.933#

W_e' = 4.31#

TABLE IX

M.I.T. PROPELLER NO. 28

DD 409

Material = Aluminum

Diameter (d) = 11.82"

No. of Blades (N) = 3

Pitch Ratio (P/D) = 1.11

Mean Width Ratio (MWR) = 0.458

dK_t/dJ $.65 < J < 1.15$ = .484

S = 881

W_p = 2.875#

W_h = 0.125#

W_l = 3.000#

W_s = 4.503#

RUN	h	t	v_o	N	J	T_o	T_o^2	W_a	W_e	α	B_a	B_s	B_e	b
114	0	-	0	0	-	.1166	.01359	11.97	4.47	3.75	2.78	.59	2.19	
115	17.5	68	1.74	150	.70	.10075	.01015	8.96	1.46	1.70	.96	.74	.22	2.24
116	39.0	68	2.60	152	1.03	*				6.62	3.72	.80	2.92	2.27
117	57.0	68	3.14	154	1.22	.1022	.01044	9.20	1.70	2.54	1.45	.82	.63	2.30
118	40.0	68	1.63	150	.65	*				5.50	3.09	.73	2.36	2.24

* Damping is too severe for period measurement.

W_a (average, operating) = 9.080#

W_e^1 = 2.72#

TABLE X

M.I.T. PROPELLER NO. 32

DD 409

Material = Aluminum

Diameter (d) = 11.82"

No. of Blades (N) = 3

Pitch Ratio (P/D) = 1.19

Mean Width Ratio (MWR) = 0.458

dK_t/dJ $.7 < J < 1.25$ = .441

S = 881

W_p = 2.780#

W_h = 0.063#

W_1 = 2.843#

W_s = 4.503#

RUN	h	t	v_o	N	J	T_o	T_o^2	W_a	W_e	a	B_a	B_s	B_e	b
123	0	-	0	0	-	.10650	.01134	10.00	2.654	3.47	2.16	.59	1.57	
124	18.5	68	1.79	149	.72	.09948	.00989	8.70	1.35	1.80	.99	.74	.25	2.03
125	38.0	68	2.57	150	1.03	.10000	.01000	8.81	1.46	2.50	1.37	.80	.57	2.04
126	57.1	68	3.15	151	1.26	.10105	.01021	9.00	1.65	3.06	1.68	.82	.86	2.06

W_a (average, operating) = 8.837#

$W_e{}'$ = 2.50#

TABLE XI

M.I.T. PROPELLER NO. 31

DD 409

Material = Aluminum

Diameter (d) = 11.82"

No. of Blades (N) = 4

Pitch Ratio (P/D) = 0.90

Mean Width Ratio (MWR) = 0.458

S = 881

W_p = 3.250#

W_h = .062#

W_l = 3.312#

W_s = 4.503#

RUN	h	t	v_o	N	J	T_o	T_o^2	W_a	W_e	α	B_a	B_s	B_e
110	0	-	0	0	-	.1294	.01675	14.76	6.945	1.90	1.74	.59	1.15
111	15.0	67.5	1.61	154	.63	.1090	.01187	10.45	2.63	1.80	1.21	.73	.48
112	36.0	67.5	2.50	150	1.00	.1107	.01226	10.79	2.97	2.28	1.53	.79	.74
113	58.5	67.5	3.18	153	1.25	.1123	.01261	11.11	3.29	2.30	1.54	.82	.72

K_t curves not available.

W_a (average, operating) = 10.783#

W_e^1 = 5.30#

TABLE XII

M.I.T. PROPELLER NO. 33

DD 409

Material = Aluminum

Diameter (d) = 11.82"

No. of Blades (N) = 4

Pitch Ratio (P/D) = 1.20

Mean Width Ratio (MWR) = 0.458

S = 881

W_p = 3.250#

W_h = 0.063#

W_l = 3.313#

W_s = 4.503#

RUN	h	t	v_o	N	J	T_o	T_o^2	W_a	W_e	α	B_a	B_s	B_e
119	0	-	0	0	-	.1275	.01626	14.31	6.494	4.12	3.67	.59	3.08
120	16.0	68	1.67	150	.67	.10565	.011162	9.85	2.03	1.78	1.07	.73	.34
121	34.5	68	2.45	152	.97	.10369	.010751	9.49	1.67	2.05	1.24	.79	.45
122	62.0	68	3.28	151	1.31	.10590	.011218	9.90	2.08	2.48	1.50	.83	.67

K_t curves not available.

W_a (average, operating) = 9.747#

W_e' = 3.26#

TABLE XIII

M.I.T. PROPELLER NO. 35

DD 409

Material = Aluminum

Diameter (d) = 8.001"

No. of Blades (N) = 3

Pitch Ratio (P/D) = 1.07

Mean Width Ratio (MWR) = 0.458

S = 907

W_p = 0.750#

W_h = 0.030#

W_l = 0.780#

W_s = 4.143#

RUN	h	t	v_o	N	J	T_o	T_o^2	W_a	W_e	α
130[1]	0	-	0	0	-	.08479	.00720	6.54	1.617	1.34
130	17.0	68	1.72	232	.44	.06695				3.30
131	18.5	68	1.79	150	.72	*				*
132	20.0	68	1.86	328	.34	.07022	.00490	4.45	-.47	3.84
133	114.5	68	4.46	330	.81	.06975				5.80
134	44.0	68	2.76	330	.50	.06896				3.60
135	11.0	68	.44	330	.08	.0712				4.80

*Damping is too severe for period measurement.

A negative W_e is not possible so this set is not included for analysis. The thrust collars were not properly seated against the bearings.

B. Sample Calculations

Torsional Coupling Factor

Derivation

1. Referring to Appendix C, Professor Lewis' unpublished notes, equation 2, we see that if we neglect the damping terms we arrive at the following:

$$\omega^4 (m_L' m_\theta - m_c^2) - \omega^2 (m_L' k_\theta + k_L m_\theta) + k_L k_\theta = 0$$

assume $m_L m_\theta = (m_L' m_\theta - m_c^2)$

where $m_L = W_a/g$ = measured apparent mass

$m_L' = \frac{W_a}{g}$ (corrected) = apparent mass corrected for torsional coupling

$m_\theta = I_p + \beta I_p'$ (effective polar inertia)

$\beta \simeq 0.25$ to include torsional virtual inertia

I_p = polar inertia of propeller being tested

I_p' = polar inertia of bronze propeller of same dimensions as actual propeller

$m_c = \frac{2\pi \beta I_p'}{p}$

p = pitch, in.

2. Suppose $k_\theta = 0$ (close to our $k_\theta = 7.34 \frac{\text{in \#}}{\text{radian}}$)

$$\omega^4 (m_L' m_\theta - m_c^2) - \omega^2 m_\theta k_L = 0$$

$$\omega_1^2 = \frac{k_L}{\frac{m_L' - m_c^2}{m_\theta}}$$

3. Suppose $k_\theta = \infty$

$$\omega_2^2 = \frac{k_L}{m_L'}$$

4. Correction of frequencies to $k_\theta = \infty$

Define C_I = torsional coupling factor

$$\frac{\omega_1^2}{\omega_2^2} = \frac{m_L'}{m_L' - \frac{m_c^2}{m_\theta}} = \frac{m_L'}{m_L} = C_I$$

Sample Calculations

1. Bronze Propeller #80 P/D = 1.2

$$I_p = \frac{0.0046}{386} nD^3bt \quad \# \text{ sec}^2 \text{ in} \qquad \text{(Reference 6)}$$

where n = no. of blades

D = diameter, in

b = maximum developed blade width, in

t = maximum developed blade thickness at 1/2 radius, axis to tip

$$b = \frac{MWR\ D}{.842} \qquad \text{(Reference 5 page 157)}$$

MWR = Mean Width Ratio

$$b = \frac{(.248)(11.90)}{.842} = 3.51 \text{ in}$$

$$I_p = \frac{0.0046}{386}(4)(11.90)^3(3.51)(\tfrac{1}{4}) = 0.0706$$

$$m_L = \frac{W_a}{g_o} = \frac{14.656}{386} = 0.0380$$

$$m_\theta = (1 + \beta)I = (1.25)(.0706) = 0.0884$$

$$m_c = \frac{2\pi\beta I}{D(P/D)} = \frac{2\pi(.25)(.0706)}{(11.90)(1.2)} = 0.00777 = \frac{0.00930}{P/D}$$

$$m_L' = m_L \left(1 + \frac{m_c^2}{m_L m_\theta}\right) = m_L C_I = m_L (1.01803)$$

$$C_I = 1.01803$$

2. Aluminum Propeller #72 $\qquad P/D = 0.9$

$$m_L = \frac{W_a}{g_o} = \frac{9.107}{386} = 0.0236$$

$$m_\theta = I_p + \beta I'_p = \left(\frac{\text{density of al.}}{\text{density of bronze}}\right) I_p' + \beta I'_p$$

$$= (0.287 + .25)(.0706) = 0.0379$$

$$m_c = \frac{0.00930}{P/D} = 0.01034$$

Torsional Coupling Factor

$$m_L' = m_L \left(1 + \frac{m_c^2}{m_L m_\theta}\right) = m_L C_I$$

$$C_I = 1.1197$$

Determination of Empirical Equation

The term for virtual mass, W_e' has four major parameters as follows:

d (diameter) (inches)

N (number of blades)

MWR (mean width ratio)

P/D (pitch ratio)

In equation form W_e' can be expressed as follows:

$$W_e' = C_{rsw} \quad f(P/D) \quad f(d) \quad f(N) \quad f(MWR) \qquad (\#)$$

where C_{rsw} is a constant.

Analysis of figure by trial and error for P/D term.

$$y = C_x^2 \quad C = y/x^2 \quad \text{where} \begin{cases} y = \dfrac{W_e'}{W_e'_{P/D=1}} - 0.600 \\ x = 1.350 - P/D \end{cases}$$

$y=.85 \quad x=.55 \quad x^2=.304$

$$C = \frac{.85}{.304} = 2.8$$

x	x^2	y
.1	.01	.028
.2	.04	.112
.3	.09	.252
.4	.16	.448
.5	.25	.700

Shift this curve up 0.04.

$$\therefore \begin{cases} y = \dfrac{W_e'}{W_e'_{P/D=1}} - 0.640 \\ x = 1.350 - P/D \end{cases}$$

This best matches plotted values.

$$\therefore \quad y = 2.80\, x^2$$

$$\frac{W_e'}{W_e'_{P/D=1}} - 0.640 = 2.80\,(1.350-P/D)^2$$

$$\frac{W_e'}{W_e'_{P/D=1}} = 2.80\,(1.350-P/D)^2 + 0.640 \qquad (2)$$

$$.75 < P/D < 1.25$$

The first term f(P/D) is of the form of equation (2). Dividing by 2.80 simplifies the expression,

$$W_e' = C_{rsw}\left[(1.350-P/D)^2 + 0.228\right] \; f(d) \; f(N) \; f(MWR)$$

The term f(d) is presumed to be (d^3) since W_e' should vary as the volume. To simplify this expression divide d, the diameter of the propeller in inches, by 10.

$$W_e' = C_{rsw}\left[(1.350-P/D)^2 + 0.228\right]\left[\left(\frac{d}{10}\right)^3\right] \; f(N) \; f(MWR)$$

The term f(N) is presumed to be in the form of N^a. This is determined from the following comparisons:

$$\frac{W_e'_{31}}{W_e'_{30}} = \frac{5.30}{4.32} = \left(\frac{4}{3}\right)^a = 1.225 \qquad a = 0.705$$

$$\frac{W_e'_{33}}{W_e'_{32}} = \frac{3.27}{2.50} = \left(\frac{4}{3}\right)^a = 1.305 \qquad a = 0.925$$

Select a = 0.8

$$W_e' = C_{rsw}\left[(1.350-P/D)^2 + 0.228\right]\left[\left(\frac{d}{10}\right)^3\right]\left[(N)^{0.8}\right] \; f(MWR)$$

The term f(MWR) is presumed to be in the form of $(MWR)^b$. This is determined from the following comparisons:

$$W_e'_{28} \text{ (corrected to 4 blades)} = (2.72)\left(\frac{4}{3}\right)^{.8} = 3.42$$

$$\frac{W_e'_{28-4}}{W_e'_{73}} = \frac{3.42}{1.70} = \left(\frac{.458}{.248}\right)^b = 2.010 \qquad b = 1.140$$

$$\frac{W'_{31}}{W'_{72}} = \frac{5.30}{2.67} = \left(\frac{.458}{.248}\right)^b = 1.985 \qquad b = 1.120$$

Select b = 1.13

Figure XXI

W_θ'/W_θ (P/D-1) vs. P/D

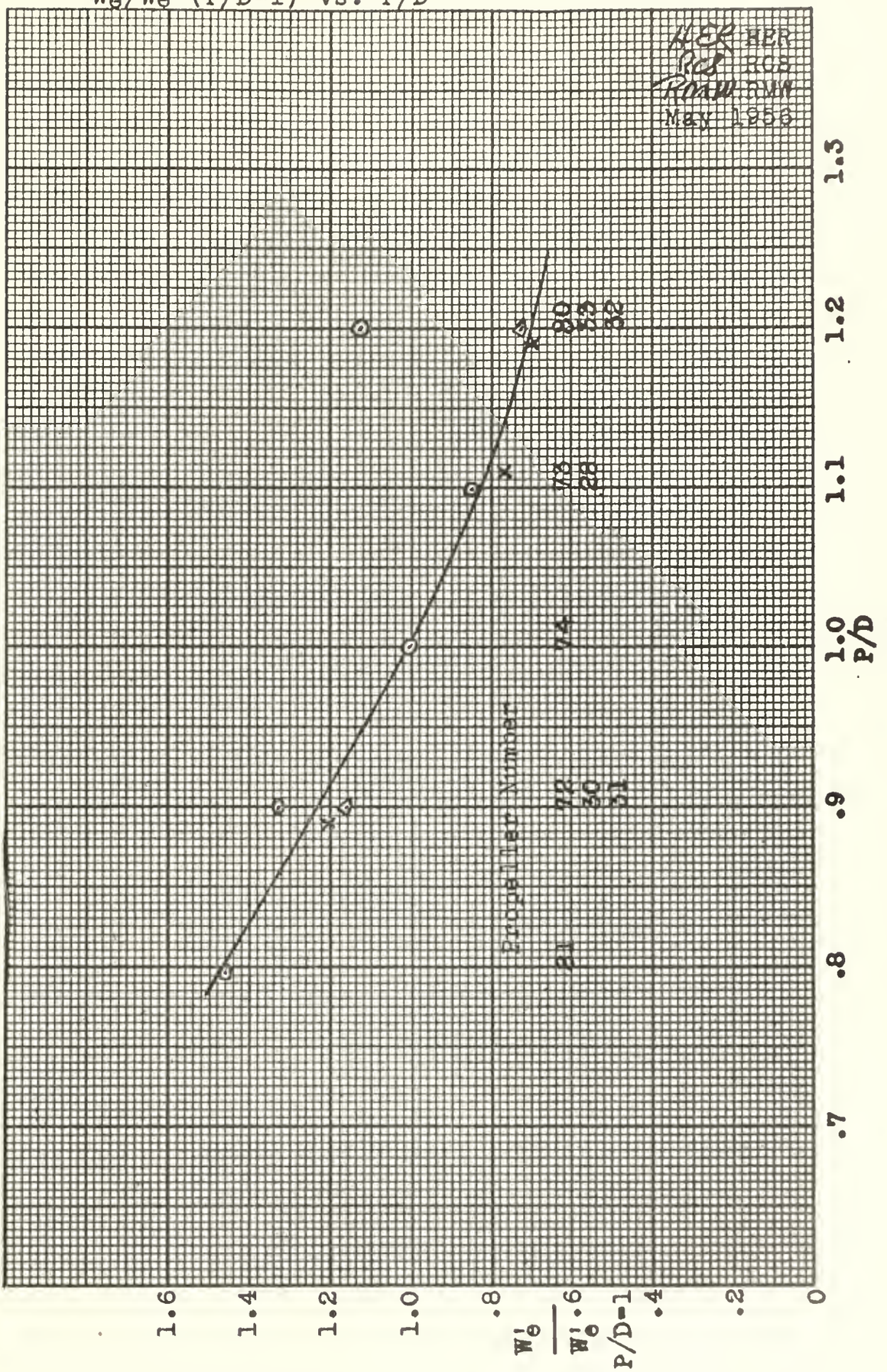

(1) $$W_e' = C_{rsw} \left[(1.350-P/D)^2 + 0.228\right] \left[\left(\frac{d}{10}\right)^3\right] \left[(N)^{0.8}\right] \left[(MWR)^{1.13}\right]$$

The value of the constant is obtained by substituting the data into equation (1).

Propeller 81

$$W_e' = C_{rsw}(.534)(1.686)(3.03)(.207) = .565\ C_{rsw}$$

Propeller 72

$$W_e' = C_{rsw}(.431)(1.686)(3.03)(.207) = .455\ C_{rsw}$$

Propeller 74

$$W_e' = C_{rsw}(.353)(1.686)(3.03)(.207) = .373\ C_{rsw}$$

Propeller 73

$$W_e' = C_{rsw}(.290)(1.686)(3.03)(.207) = .306\ C_{rsw}$$

Propeller 80 — W_e' is obviously too high.

Propeller 30

$$W_e' = C_{rsw}(.439)(1.651)(2.41)(.414) = .723\ C_{rsw}$$

Propeller 28

$$W_e' = C_{rsw}(.281)(1.651)(2.41)(.414) = .463\ C_{rsw}$$

Propeller 32

$$W_e' = C_{rsw}(.2536)(1.651)(2.41)(.414) = .418\ C_{rsw}$$

Propeller 31

$$W_e' = C_{rsw}(.431)(1.651)(3.03)(.414) = .894\ C_{rsw}$$

Propeller 33

$$W_e' = C_{rsw}(.2505)(1.651)(3.03)(.414) = .520\ C_{rsw}$$

Prop. No.	W_e'	$\frac{W_e'}{C_{rsw}}$	C_{rsw}	W_e' (equation, $C_{rsw} = 5.773$
81	2.94	.565	5.19	3.26
72	2.68	.455	5.87	2.63
74	1.99	.373	5.33	2.15
73	1.70	.306	5.56	1.77
80	2.25			
30	4.31	.723	5.96	4.18
28	2.72	.463	5.87	2.67
32	2.50	.418	5.98	2.41
31	5.30	.894	5.93	5.16
33	3.26	.520	6.27	3.00

$$C_{rsw_{av}} = \frac{51.96}{9} = 5.773$$

(1) $$W_e' = 5.773 \left[(1.350-P/D)^2 + 0.228\right] \left[\left(\frac{d}{10}\right)^3\right] \left[(N)^{0.8}\right] \left[(MWR)^{1.13}\right]$$

$$.750 < P/D < 1.25$$

Derivation of Simple Damping Constant

b = damping constant $(\frac{\#\ sec}{ft})$

K_t = thrust coefficient

T = thrust (lbf)

ρ = density $(\frac{lbf\ sec^2}{ft^4})$ = 1.938 for F.W.

n = revolutions per second

$$b = \frac{dT}{dv_o}$$

$$K_t = \frac{T}{\rho n^2 D^4} \qquad T = \rho n^2 D^4 K_t$$

$$J = \frac{v_o}{nD} \qquad v_o = JnD$$

$$b = \frac{dT}{dv_o} = \frac{\rho n^2 D^4}{nD} \frac{dK_t}{dJ} = \rho nD^3 \frac{dK_t}{dJ}$$

In the above ∂ (partial derivative of) is indicated by d.

C. EXTRACT FROM UNPUBLISHED PAPER

THE COUPLING OF LONGITUDINAL AND TORSIONAL VIBRATION OF MARINE PROPELLER SHAFTING

Unpublished paper by 23 February 1954

Frank M. Lewis, Professor, Massachusetts Institute of Technology

The longitudinal and torsional oscillations of marine propulsion systems are ordinarily calculated on the assumption that they are independent phenomena. In actuality they are coupled through the intermediary of the water reactions, so that a torsional excitation produces both longitudinal and torsional motion, and longitudinal excitation does likewise.

If the longitudinal and torsional frequencies are well removed from each other this coupling effect will be of only small importance, but if a longitudinal and a torsional frequency are close or coincide, the effect is very important altering both the position and amplitude of the criticals. Anticipating the results to a certain extent it is noted that for coincidence of the frequencies the virtual inertia and the hydrodynamic damping vanish for both longitudinal and torsional vibration. That this should be so is obvious on consideration. Assume a propeller consisting of helicoidal surfaces of zero thickness. For equal longitudinal and torsional frequencies a possible mode of vibration consists of a coupled torsional and longitudinal motion in which the propeller screws itself back and forth through the water. There would be zero virtual inertia for such a motion and the damping would be limited to surface friction, a very small effect. While for a propeller of finite thickness the inertia and damping effects

would not actually vanish, they would become small.

Passing to the derivation of the general relationships it is noted that there are two types of coupling, virtual inertia coupling and damping coupling.

The Virtual Inertia Coupling

There are three virtual inertia factors, these are:

The virtual inertia for pure torsional motion, the virtual inertia for pure longitudinal motion and the coupling virtual inertia. These are not independent factors and an approximate relationship between them can be derived as follows:--

Assume a propeller consisting of helicoidal surfaces. In Fig. (1) let A B be a blade element at angle to the plane of the propeller.

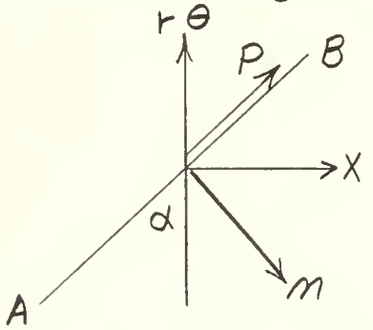

Let this be given a longitudinal displacement and a tangential displacement r θ. Resolving these into components parallel and perpendicular to the blade elements, there is found to be a normal displacement

$$n = x \cos\alpha - r\,\theta \sin\alpha$$

and a parallel

$$p = x \sin\alpha + r\,\theta \cos\alpha$$

Only the normal motion will have virtual inertia attached to it so that the normal force can be written:

$$dF_n = (dm + dm')\ddot{n}$$

and the parallel force

$$dF_p = dm\dot{p}$$

where dm and dm' are the inertia mass in air and the virtual water mass associated with a blade element. Further resolving F_n and F_p into forces parallel and perpendicular to the axis there is found.

$$dF_x = dF_n \cos\alpha + dF_p \sin\alpha$$

$$dQ = rdF_\theta = rdF_p \cos\alpha - rdF_n \sin\alpha$$

substituting and reducing there is obtained

$$dF_x = dm\ddot{x} + dm' (\cos^2\alpha\,\ddot{x} - \sin\alpha\cos\alpha\, r\ddot{\theta})$$

$$dQ = dmr^2\ddot{\theta} + dm' (\sin^2\alpha\, r^2\,\ddot{\theta} - r\sin\alpha\cos\alpha\,\ddot{x})$$

Summing overall elements.

$$F_x = m\ddot{x} + \ddot{x}\sum dm' \cos^2\alpha - \ddot{\theta}\sum dm'\, r\cos\alpha\sin\alpha$$

$$Q = I\ddot{\theta} - \ddot{x}\sum dm'\, r\sin\alpha\cos\alpha + \ddot{\theta}\sum r^2 \sin^2\alpha\, dm'$$

where m and I are the mass and polar inertia constants W/g, J/g of the propeller in air, but excluding the hub.

Considering the torque expression we note that if $\ddot{x} = 0$ there is pure torsional motion. It is known then that the virtual inertia is equivalent to an increase of the polar inertia of the propeller of the order of 25%. Let this fraction be β. This method of expressing the virtual inertia as a fraction of the propeller inertia in air is crude but will suffice for the moment.

There is thus obtained

$$dm'\, r^2 \sin^2\alpha = \beta I$$

Still considering the torque equation it is noted that the virtual inertia terms must vanish if $\dot{x}$ and $\dot{\theta}$ are so related that the propeller moves parallel to its helicoidal surface. This condition is expressed by

$$\frac{\ddot{x}}{\ddot{\theta}} = \frac{p}{2\pi}$$

where P is the pitch. Equating the dm' terms to zero with this relationship there is obtained

$$\sum dm' \; r \sin\alpha \cos\alpha = \frac{2\pi\beta I}{p}$$

considering the F_x expression the dm' terms must likewise vanish if

$$\frac{\ddot{x}}{\ddot{\theta}} = \frac{p}{2}$$

This leads to

$$\sum dm' \cos^2\alpha = \frac{2\pi}{p}\sum dm' \; r \sin\alpha \cos\alpha = \frac{4\pi^2\beta I}{p^2}$$

This should be the virtual inertia for a pure longitudinal motion. Insertion of numerical values shows that it comes very close to the .5 value, in itself a very crude approximation, which is ordinarily assumed. The expressions for the longitudinal force and the torque now become

$$F_x = \left(m + \frac{4\pi^2\beta I}{p^2}\right)\ddot{x} - \frac{2\pi\beta I}{p}\ddot{\theta}$$

$$Q = I(1+\beta)\ddot{\theta} - \frac{2\pi\beta I}{p}\ddot{x}$$

These are the final expressions for the inertia forces associated with the propeller.

For pure longitudinal and torsional motion these reduce to the values ordinarily used and the virtual inertia component becomes zero for motion parallel to the helicoidal surface.

The expressions can be more conveniently written

$$F_x = m_L \ddot{x} - m_c \ddot{\theta}$$

$$Q = m_\theta \ddot{\theta} - m_c \ddot{x}$$

when m_L, m_θ, m_c are the longitudinal, torsional, and coupling inertia coefficients respectively.

It is now assumed that there exists a simple harmonic longitudinal motion x of frequency ω superposed upon a rotary simple harmonic motion θ of frequency ω. Exciting forces and torques F_e and Q_e of frequency ω likewise act. With k_L and k_θ as the longitudinal and torsional spring constants and neglecting damping the vector force and torque equations for a single mass system are:--

$$F_e - k_L x + m_L \omega^2 x - m_c \omega^2 \theta = 0$$

$$Q_e - k_\theta \theta + m_\theta \omega^2 \theta - m_c \omega^2 x = 0$$

These equations have the solution

$$x = \frac{F_e}{\Delta}(k_\theta - m_\theta \omega^2) + \frac{Q_e}{\Delta}(-m_c \omega^2)$$

$$\theta = \frac{Q_e}{\Delta}(k_L - m_L \omega^2) + \frac{F_e}{\Delta}(-m_c \omega^2)$$

where $$\Delta = \omega^4 (m_L m_\theta - m_c^2) - \omega^2 (m_L k_\theta + k_L m_\theta) + k_L k_\theta \qquad (2)$$

The 2 natural frequencies of the system are given by the roots of the above equation, i.e. $\Delta = 0$.

With the substitutions

$$m_L = m + \frac{4\pi^2 \beta I}{p^2}$$

$$m_\theta = I(1 + \beta)$$

$$m_c = \frac{2\pi \beta I}{p}$$

The frequency equation reduces to

$$\omega^4 \left[I(1+\beta)m + \frac{4\pi^2}{p^2} \beta I^2 \right]$$

$$- \omega^2 \left[k_\theta \left(m + \frac{4\pi^2}{p^2} \beta I \right) + k_L I(1+\beta) \right] + k_L k_\theta = 0$$

Considering the $\Delta = 0$ equation as applied to a single degree of freedom system it is evident that in the absence of the coupling term the roots would be $\omega_L^2 = \frac{k_L}{m_L}$ and $\omega_\theta^2 = \frac{k_\theta}{m_\theta}$ i.e., the separate longitudinal and torsional frequencies with water inertia included. One of these will be higher than the other. The effect of the coupling inertia m_c is to lower the lowest of the two frequencies and raise the higher. It will be usual in marine installations for the lowest torsional mode to occur at a much lower frequency than that of the lowest longitudinal mode.

(Author's Note:

The above is a liberal extract from the original paper by Professor Frank M. Lewis. It is hoped that there has been no distortion of the contents by using for the most part only those portions of the paper which dealt with our problem.)

APPENDIX D.

Instrumentation Data

Recorder. Sanborn 150

Model 152-1100 Serial number 18.

Gages. SR4, Baldwin Lima Hamilton

Type A-7

Resistance 120.0 ± 0.3 ohms

Gage Factor 1.91 ± 2%

Lot No. 232 - 11B72

APPENDIX E. BIBLIOGRAPHY

1. Kane, J. R. and McGoldrick, R. T. "Longitudinal Vibration of Marine Propulsion-Shafting Systems", Transactions of the Society of Naval Architects and Marine Engineers, Volume 57, 1949, pp 193-231

2. Lamb, H., Hydrodynamics (sixth edition), pp 150-154

3. Lewis, F. M., "Propeller Tunnel Notes", Transactions of the Society of Naval Architects and Marine Engineers, Volume 55, 1947, pp 284-295

4. Lewis, F. M., "The Coupling of Longitudinal and Torsional Vibration of Marine Propeller Shafting", Unpublished paper, 1954

5. Rossell, H. E. and Chapman, L. B., Principles of Naval Architecture, Volume II, First Edition 1939, pp 138-157

6. Seward, H. L., Marine Engineering, Volume II, First Edition 1942, pp 84-86, 98-99

7. David Taylor Model Basin Report 518, March 1945, "Analysis of Vibration in the Propelling Machinery of the Battleships NORTH CAROLINA and WASHINGTON

8. Hughes, W. L., "Propeller Blade Vibrations", Transactions North East Coast Institution of Engineers and Shipbuilders, Volume 65, 1948-1949

Thesis
R898

28920

Russell
The determination of
longitudinal virtual mass and
damping of a rotating propeller